

# Delaunay surfaces of prescribed mean curvature in homogeneous 3-spaces

Antonio Bueno

Departamento de Geometría y Topología, Universidad de Granada, E-18071 Granada, Spain.  
*E-mail address:* jabueno@ugr.es

## Abstract

We obtain a classification result for rotational surfaces in the homogeneous 3-spaces with 4-dimensional isometry group, whose mean curvature is given as a prescribed  $C^1$  function depending on their angle function. Under necessary and sufficient geometric hypothesis on the prescribed function, we show that these surfaces behave likely the Delaunay surfaces of constant mean curvature. In contrast with the constant mean curvature case, in the Heisenberg space and in the universal cover of the special linear group, we exhibit the existence of rotational prescribed mean curvature tori.

## 1 Introduction

A fundamental problem in classic Differential Geometry is the study of surfaces in the Euclidean space  $\mathbb{R}^3$  whose principal curvatures and Gauss map satisfy a prescribed relation. In this general setting, two of the main theories are the one of surfaces with positive constant mean curvature (CMC surfaces in the following), and the one of *Minkowski-type prescribed curvature problems*.

In the past decades, the theory of CMC surfaces has been extended to further ambient frameworks, being of remarkable importance the so-called  $\mathbb{E}(\kappa, \tau)$  spaces: the homogeneous, simply connected 3-dimensional manifolds whose isometry group have dimension greater than three and are not space forms. One of the major achievements was the resolution of the Hopf problem by Abresch-Rosenberg [AbRo1, AbRo2], proving that the only immersed CMC spheres are the rotational ones. This milestone attracted the attention of many researches, becoming an active field of research; see e.g. [Dan, DHM, FeMi] and references therein for an outline of the development of this theory.

Regarding prescribed curvature problems, the existence and uniqueness of surfaces defined by a prescribed relation between its principal curvatures and its Gauss map goes back, at least, to the famous Minkowski and Christoffel problems for ovaloids [Min, Chr]. When such prescribed relation is the average of the principal curvatures, i.e. we prescribe the mean curvature, the following class of immersed surfaces in  $\mathbb{R}^3$  arises as a very particular case:

---

*Mathematics Subject Classification:* 53A10, 53C42, 34C05, 34C40

*Keywords:* Prescribed mean curvature, Homogeneous 3-spaces, Delaunay-type classification result; Rotational tori.

**Definition 1.1** *Let be  $\mathcal{H} \in C^1(\mathbb{S}^2)$ . An immersed, oriented hypersurface  $\Sigma$  in  $\mathbb{R}^3$  has prescribed mean curvature  $\mathcal{H}$  if its mean curvature function  $H_\Sigma$  is given by*

$$H_\Sigma(p) = \mathcal{H}(N_p), \quad \forall p \in \Sigma,$$

where  $N : \Sigma \rightarrow \mathbb{S}^2$  is the Gauss map of  $\Sigma$ .

For short, we say that  $\Sigma$  is an  $\mathcal{H}$ -surface. Recall that for  $\mathcal{H} = H_0$  a constant we have surfaces with CMC equal to  $H_0$ , and for  $\mathcal{H}(N) = \langle N, e_3 \rangle$  we have the translating solitons.

Among others, Alexandrov and Pogorelov in the '50s [Ale, Pog] and more recently Guan-Guan [GuGu] and Gálvez-Mira [GaMi1, GaMi2, GaMi3], focused on the existence and uniqueness of immersed  $\mathcal{H}$ -spheres. Recently, the author jointly with Gálvez and Mira started to develop the *global theory of surfaces with prescribed mean curvature* in [BGM1, BGM2], taking as starting point the well-studied theory of CMC surfaces in  $\mathbb{R}^3$ .

For further results on  $\mathcal{H}$ -surfaces, see [Bue1] for the resolution of the Björling problem in  $\mathbb{R}^3$ ; [Bue2] for the obtention of half-space theorems for properly immersed  $\mathcal{H}$ -surfaces in  $\mathbb{R}^3$ ; and [BuOr] for the study of invariant hypersurfaces with *linear* prescribed mean curvature in  $\mathbb{R}^{n+1}$ .

As pointed out by the authors in Remark 2.4 in [BGM2], the  $\mathcal{H}$ -surfaces can be defined in a general Lie group endowed with a left-invariant metric, where we can prescribe a function  $\mathcal{H}$  in the unit sphere  $\mathbb{S}_\mathfrak{g}^2$  of the Lie algebra  $\mathfrak{g}$ . Then, in Definition 1.1 we take the left-invariant Gauss map in order to define the prescribed mean curvature problem, see [GaMi1, GaMi3]. Regarding the  $\mathbb{E}(\kappa, \tau)$  spaces we find out to difficulties when trying to extend Definition 1.1. First:  $\mathbb{S}^2(\kappa) \times \mathbb{R}$  does not carry a Lie group structure, opposite to the remaining  $\mathbb{E}(\kappa, \tau)$  spaces; and second: the same space can inherit two non-isometric Lie group structures: one unimodular and other non-unimodular; for instance, this happens for the space  $\mathbb{H}^2(\kappa) \times \mathbb{R}$ , see [MePe] for details.

In this paper we restrict ourselves to immersed surfaces whose mean curvature is a prescribed function depending on the *angle function*:

**Definition 1.2** *Let be  $\mathfrak{h} \in C^1([-1, 1])$ . An immersed, oriented surface  $\Sigma$  in  $\mathbb{E}(\kappa, \tau)$  has prescribed mean curvature  $\mathfrak{h}$  if its mean curvature function  $H_\Sigma$  is given by*

$$H_\Sigma(p) = \mathfrak{h}(\langle \eta_p, \xi \rangle), \quad \forall p \in \Sigma, \tag{1.1}$$

where  $\eta : \Sigma \rightarrow T\mathbb{E}(\kappa, \tau)$  is the unit normal vector field on  $\Sigma$ ,  $\xi$  is the vertical Killing vector field in  $\mathbb{E}(\kappa, \tau)$  and  $\langle \eta_p, \xi \rangle =: \nu_p$  is the so-called angle function of  $\Sigma$ .

For short, we will say that  $\Sigma$  is an  $\mathfrak{h}$ -surface. Again, we point out that for certain choices of the prescribed function, the  $\mathfrak{h}$ -surfaces have already appeared in the literature:

- If  $\mathfrak{h} = H_0 \in \mathbb{R}$ , then the  $\mathfrak{h}$ -surfaces in  $\mathbb{E}(\kappa, \tau)$  are just the surfaces with constant mean curvature equal to  $H_0$ .

- If  $\mathfrak{h}(y) = y$ ,  $\forall y \in [-1, 1]$ , the mean curvature is given by  $H_\Sigma(p) = \nu_p$ , i.e. is the angle function. These surfaces correspond to translating solitons of the mean curvature flow for the Killing vector field  $\xi$ , and its study has started in  $\mathbb{M}^2(\kappa) \times \mathbb{R}$  [LiMa] and  $\text{Nil}_3$  [Pip].

Note that if  $\mathbb{E}(\kappa, \tau)$  is non-isometric to  $\mathbb{S}^2(\kappa) \times \mathbb{R}$ , the  $\mathfrak{h}$ -surfaces arise when we prescribe a function  $\mathcal{H} \in C^1(\mathbb{S}_g^2)$  that is *rotationally symmetric*, i.e. it only depends on the height in  $\mathbb{S}_g^2$  measured in the  $\xi$ -direction.

Among the classical results in the CMC surface theory in  $\mathbb{R}^3$ , one of the most celebrated is the classification due to Delaunay of the complete, rotational CMC surfaces as round spheres, cylinders, unduloids and nodoids. In the literature, these surfaces are commonly known as *Delaunay surfaces*.

Regarding CMC surfaces in the  $\mathbb{E}(\kappa, \tau)$  spaces, a similar classification result has been achieved in the product spaces  $\mathbb{M}^2(\kappa) \times \mathbb{R}$  by [HsHs, PeRi], in the Heisenberg space  $\text{Nil}_3$  by [Tom], in the universal cover of the special linear group  $\widetilde{SL}_2(\mathbb{R})$  by [Gor, Tor] and in the Berger spheres  $\mathbb{S}_b^3(\kappa, \tau)$  by [Tor]. If the constant mean curvature  $H_0$  satisfies  $4H_0^2 + \kappa > 0$ , the rotational CMC surfaces roughly behave as the Delaunay surfaces in  $\mathbb{R}^3$ . The value  $\sqrt{-\kappa}/2$  for  $\kappa < 0$  is known as the *critical value*; there exists a rotational sphere with CMC equal to  $H_0$  if and only if  $H_0 > \sqrt{-\kappa}/2$ . For  $H_0 \leq \sqrt{-\kappa}/2$ , entire graphs are the canonical, rotational examples intersecting orthogonally the axis of rotation.

We must emphasize that only for the case  $\kappa > 0$ , there exist rotational CMC tori. Otherwise, i.e. for  $\kappa \leq 0$ , no rotational CMC tori exist. Note that only for  $\tau = 0$  this is trivial by applying Alexandrov's reflection technique with respect to vertical planes.

For prescribed mean curvature surfaces in  $\mathbb{R}^3$ , a *Delaunay-type classification result* was exhibited in [BGM1]. Under necessary and sufficient assumptions on  $\mathcal{H} \in C^1(\mathbb{S}^2)$ , the authors proved that the rotational examples behave the same as the classical Delaunay surfaces in  $\mathbb{R}^3$ . As a matter of fact, no rotational  $\mathcal{H}$ -tori exist. The arbitrariness of  $\mathcal{H}$  made hopeless to find a first integral of the system of ODE's obtained from the condition of being rotationally invariant, even for concrete choices. Instead, the authors analyzed the geometric properties of rotational  $\mathcal{H}$ -surfaces by means of a *phase plane* analysis.

Inspired by the Delaunay-type classification results for CMC surfaces in the  $\mathbb{E}(\kappa, \tau)$  spaces and for  $\mathcal{H}$ -surfaces in  $\mathbb{R}^3$ , in this paper we obtain a classification result for complete, rotational  $\mathfrak{h}$ -surfaces in the  $\mathbb{E}(\kappa, \tau)$  spaces, assuming that the prescribed function  $\mathfrak{h}$  belongs to the space of functions  $\mathfrak{C}^1$ , where

$$\mathfrak{C}^1 := \{\mathfrak{h} \in C^1([-1, 1]); \mathfrak{h}(y) = \mathfrak{h}(-y) > 0 \text{ and } 4\mathfrak{h}(y)^2 + \kappa(1 - y^2) > 0, \forall y \in [-1, 1]\}. \quad (1.2)$$

Note that for the particular case that  $\mathfrak{h}$  is a constant  $H_0 > 0$  and  $\kappa < 0$ , the fact that  $H_0 \in \mathfrak{C}^1$  reads as  $H_0 > \sqrt{-\kappa}/2$ .

Our main result is the following Delaunay-type classification result for  $\mathfrak{h}$ -surfaces:

**Theorem 1.3** *Let be  $\mathfrak{h} \in \mathfrak{C}^1$ . Up to vertical translations, any complete, rotational  $\mathfrak{h}$ -surface in the space  $\mathbb{E}(\kappa, \tau)$  is one of the following:*

1. The vertical cylinder with radius  $x_0 = 2 \left( \sqrt{4\mathfrak{h}(0)^2 + \kappa} + 2\mathfrak{h}(0) \right)^{-1}$  and constant mean curvature  $\mathfrak{h}(0)$ . In  $\mathbb{S}_b^3(\kappa, \tau)$ , this cylinder is a compact CMC torus.
2. An embedded  $\mathfrak{h}$ -sphere with strictly monotone angle function.
3. A 1-parameter family of properly embedded  $\mathfrak{h}$ -unduloids.
4. A 1-parameter family of properly immersed (with self-intersections)  $\mathfrak{h}$ -nodoids.
5. An embedded  $\mathfrak{h}$ -torus in the space  $\mathbb{S}^2(\kappa) \times \mathbb{R}$ .
6. An  $\mathfrak{h}$ -surface in  $\mathbb{S}_b^3(\kappa, \tau)$  generated by rotating a union of curves meeting at a point of the antipodal fiber of the rotation axis.

One of the major issues, which is a huge difference between  $\mathfrak{h}$ -surfaces and CMC surfaces, is that the profile curve of the  $\mathfrak{h}$ -nodoids of type 4. in Theorem 1.3 may be closed in  $\mathbb{E}(\kappa, \tau)$  spaces with  $\kappa \leq 0$ . This configuration would lead to the existence of rotational embedded  $\mathfrak{h}$ -tori, providing counterexamples to the Alexandrov problem for  $\mathfrak{h}$ -surfaces.

In general, the Alexandrov problem for a class of surfaces  $\mathcal{A}$  immersed in some ambient space  $\mathcal{M}$  asks whether a compact and embedded surface  $\Sigma \in \mathcal{A}$  is topologically a sphere. When  $\mathcal{A}$  is the class of CMC surfaces and  $\mathcal{M}$  is  $\mathbb{R}^3$  this was originally proved by Alexandrov applying his celebrated argument of moving planes.

However, the situation changes when  $\mathcal{M}$  is an  $\mathbb{E}(\kappa, \tau)$  space. For  $\kappa > 0$ , rotational CMC tori exist. For  $\kappa < 0$  and  $\tau = 0$ , i.e. in  $\mathbb{H}^2(\kappa) \times \mathbb{R}$ , we can apply Alexandrov reflection technique with respect to vertical planes and conclude that a compact and embedded CMC surface is a topological sphere, and by the classification of Abresch-Rosenberg it must be the rotational canonical example. When  $\kappa \leq 0$  and  $\tau \neq 0$ , i.e. in the spaces  $\text{Nil}_3$  and  $\widetilde{SL}_2(\mathbb{R})$ , the Alexandrov problem is still an outstanding open problem in the CMC theory.

Regarding  $\mathfrak{h}$ -surfaces in the  $\mathbb{E}(\kappa, \tau)$  spaces, Theorem 1.3 yields that rotational  $\mathfrak{h}$ -tori exist when  $\kappa > 0$ . If  $\kappa < 0$  and  $\tau = 0$ , no rotational  $\mathfrak{h}$ -tori can exist in  $\mathbb{H}^2(\kappa) \times \mathbb{R}$  in virtue of Alexandrov reflection technique with respect to vertical planes; these isometries are induced as isometries for  $\mathfrak{h}$ -surfaces as explained in Section 2. The main difference here is that for  $\kappa \leq 0$  and  $\tau \neq 0$ , we give sufficient conditions for the non-existence of rotational  $\mathfrak{h}$ -tori and also ensure the existence of rotational  $\mathfrak{h}$ -tori for rather choices of the prescribed function  $\mathfrak{h} \in \mathcal{C}^1$ :

**Theorem 1.4** *Let be  $\mathfrak{h} \in \mathcal{C}^1$ .*

1. *If  $\mathfrak{h}$  is non-increasing in  $[-1, 0]$ , then there do not exist rotational  $\mathfrak{h}$ -tori in  $\text{Nil}_3$  and  $\widetilde{SL}_2(\mathbb{R})$ .*
2. *There are choices of  $\mathfrak{h}$  such that there exist rotational embedded  $\mathfrak{h}$ -tori in  $\text{Nil}_3$  and  $\widetilde{SL}_2(\mathbb{R})$ .*

Note that a constant  $\mathfrak{h} = H_0 \in \mathcal{C}^1$  lies in the hypothesis of Item 1., recovering the non-existence of rotational CMC tori in  $\mathbb{H}^2(\kappa) \times \mathbb{R}$ ,  $\text{Nil}_3$  and  $\widetilde{SL}_2(\mathbb{R})$ .

These rotational and embedded  $\mathfrak{h}$ -tori provide counterexamples to Alexandrov problem for  $\mathfrak{h}$ -surfaces in these  $\mathbb{E}(\kappa, \tau)$  spaces, that is, the rotational embedded  $\mathfrak{h}$ -spheres given by Item 1. of Theorem 1.3 are not unique in Alexandrov sense.

The rest of the introduction is devoted to further detail the organization of the paper.

In Section 2 we define the  $\mathbb{E}(\kappa, \tau)$  spaces as the family of 3-dimensional homogeneous manifolds with a 4-dimensional isometry group, and we introduce a canonical coordinate model. We also define the class of immersed  $\mathfrak{h}$ -surfaces in  $\mathbb{E}(\kappa, \tau)$  and deduce some properties, making special emphasis on the ambient isometries that are induced as isometries for  $\mathfrak{h}$ -surfaces.

In Section 3 we focus in the analysis of rotational  $\mathfrak{h}$ -surfaces. In the same fashion as in [BGM1], the approach will be done by means of a phase plane study of the solutions of the non-linear, autonomous system of ODE's that the coordinates of the profile curve satisfy. In Section 3.1 we deduce the formulas that the profile curve satisfies, and relate the geometry of this curve with the prescribed mean curvature. In Section 3.2 we define the phase plane and exhibit some of its first elements. Sections 3.3 and 3.4 are devoted to study in detail the local and global properties of this phase plane. Depending on the particular geometry of the corresponding  $\mathbb{E}(\kappa, \tau)$  space, the structure of the phase plane changes, hence a detailed study must be carried out in each case.

In Section 4 we focus on the particular geometry of the  $\mathbb{E}(\kappa, \tau)$  spaces that have  $\kappa > 0$ . The coordinate model introduced in Section 2 misses to cover a fiber in each space, hence is just local. This has strong influence in the behavior of the solutions and the structure of each phase plane. For instance, the main issue is to analyze whether a solution approaches to the *antipodal* fiber of rotation.

Section 5 is devoted to the analysis of Delaunay  $\mathfrak{h}$ -surfaces. In Section 5.1 we prove Theorem 1.3 and in Section 5.2 we discuss the embeddedness and compactness of the Delaunay  $\mathfrak{h}$ -surfaces in the Berger spheres. Finally, in Section 6 we prove Theorem 1.4, where we discuss the existence of rotational  $\mathfrak{h}$ -tori in the spaces  $\text{Nil}_3$  and  $\widetilde{SL}_2(\mathbb{R})$ . In Section 6.1 we give sufficient conditions on the prescribed function  $\mathfrak{h}$  for the non-existence of rotational  $\mathfrak{h}$ -tori, while in Section 6.2 we exhibit the existence of  $\mathfrak{h}$ -tori.

**Acknowledgments:** The author is thankful to José A. Gálvez, José M. Manzano and Francisco Torralbo for helpful comments and observations.

## 2 Immersed $\mathfrak{h}$ -surfaces in the $\mathbb{E}(\kappa, \tau)$ spaces

**2.1 The  $\mathbb{E}(\kappa, \tau)$  spaces.** Consider a homogeneous, simply connected, 3-dimensional manifold whose isometry group has dimension greater than 3. Moreover, suppose that is not a space form. Then, its isometry group has dimension 4 and is one of the  $\mathbb{E}(\kappa, \tau)$  spaces for some  $\kappa, \tau \in \mathbb{R}$  such that  $\kappa \neq 4\tau^2$ . A change in the orientation in the space changes  $\tau$  into  $-\tau$ , hence we will suppose that  $\tau > 0$  without losing generality.

The  $\mathbb{E}(\kappa, \tau)$  spaces admit a Riemannian submersion  $\pi : \mathbb{E}(\kappa, \tau) \rightarrow \mathbb{M}^2(\kappa)$  onto the complete, simply connected surface of constant curvature  $\kappa$ . This fibration has a unitary Killing vector field that will be denoted by  $\xi$ , whose integral curves are precisely the fibers of the

submersion; recall that the fibers are the sets  $\pi^{-1}(q)$ ,  $q \in \mathbb{M}^2(\kappa)$ . The group of isometries generated by the Killing vector field  $\xi$  are the *vertical translations*.

If  $\tau = 0$  we recover the product spaces  $\mathbb{M}^2(\kappa) \times \mathbb{R}$  and the submersion  $\pi$  is isomorphic to the projection  $\mathbb{M}^2(\kappa) \times \mathbb{R} \rightarrow \mathbb{M}^2(\kappa)$ . When  $\tau > 0$  we get the Heisenberg space  $\text{Nil}_3$  for  $\kappa = 0$ ; the Berger spheres  $\mathbb{S}_b^3(\kappa, \tau)$  for  $\kappa > 0$ ; and the universal cover of the special linear group, the space  $\widetilde{SL}_2(\mathbb{R})$ , for  $\kappa < 0$ . Note that in the Berger spheres, the projection  $\pi$  is isomorphic to the Hopf fibration.

A key feature is that for every  $p \in \mathbb{E}(\kappa, \tau)$  there exists a continuous 1-parameter family of orientation preserving isometries leaving pointwise fixed the fiber  $\pi^{-1}(\pi(p))$ ; these isometries will be called *rotations around the axis*  $\pi^{-1}(\pi(p))$ .

Next we describe a coordinate model for the  $\mathbb{E}(\kappa, \tau)$  spaces; when  $\kappa \leq 0$  the model is global, and when  $\kappa > 0$  the model is homeomorphic to the universal cover of the space minus one fiber. The notation used is inspired by Section 2.1. in [GaMi3]. We consider  $\mathcal{R}(\kappa, \tau)$  to be the space  $\mathbb{R}^3$  if  $\kappa \geq 0$ , or the disk  $\mathbb{D}(2/\sqrt{-\kappa})$  if  $\kappa < 0$ , endowed with coordinates  $(x, y, z)$ , and the metric

$$\langle \cdot, \cdot \rangle = \lambda^2(dx^2 + dy^2) + (\lambda\tau(ydx - xdy) + dz)^2, \quad \lambda = \frac{4}{4 + \kappa(x^2 + y^2)}. \quad (2.1)$$

Then,  $\mathcal{R}(\kappa, \tau)$  is isometric to the corresponding  $\mathbb{E}(\kappa, \tau)$  space, and the Riemannian submersion is isomorphic to the projection onto the first two coordinates. The vector fields

$$E_1 = \frac{1}{\lambda}\partial_x - \tau y\partial_z, \quad E_2 = \frac{1}{\lambda}\partial_y + \tau x\partial_z, \quad E_3 = \xi = \partial_z$$

are an orthonormal frame. The  $E_3$ -axis is defined to be the fiber  $\pi^{-1}(\pi((0, 0, 0)))$ . In this coordinate model we have that the usual rotations

$$(x, y, z) \longmapsto (x \cos \theta + y \sin \theta, -x \sin \theta + y \cos \theta, z), \quad \theta \in \mathbb{R},$$

are the rotations around the  $E_3$ -axis.

When  $\kappa > 0$ , the coordinates  $(x, y)$  are the inverse of the stereographic projection  $\Phi : \mathbb{R}^2 \rightarrow \mathbb{S}^2(2/\sqrt{\kappa}) - \{q\}$ , while the  $z$ -coordinate is the unit speed of the fiber  $\pi^{-1}(\Phi(x, y))$ . Recall that with this identification, the  $E_3$ -axis in  $\mathcal{R}(\kappa, \tau)$  is just the fiber passing through the antipodal point  $-q$ .

Note also that the base  $\mathbb{M}^2(\kappa)$  when  $\kappa \leq 0$ , or  $\mathbb{M}^2(\kappa) - \{p\}$  when  $\kappa > 0$ , is identified with the section  $\{z = 0\}$ . When  $\tau = 0$ , this section is isometric to  $\mathbb{M}^2(\kappa)$  (or  $\mathbb{S}^2(\kappa) - \{q\}$  if  $\kappa > 0$ ) and is a totally geodesic surface in  $\mathcal{R}(\kappa, \tau)$ .

Given an immersed surface  $\Sigma$  in  $\mathbb{E}(\kappa, \tau)$  and  $\eta : \Sigma \rightarrow T\mathbb{E}(\kappa, \tau)$  a unit normal along  $\Sigma$ , the function defined by

$$\nu : \Sigma \rightarrow \mathbb{R}, \quad \nu_p = \langle \eta_p, E_3 \rangle \quad (2.2)$$

is the so called *angle function* of  $\Sigma$ .

**2.2.  $\mathfrak{h}$ -surfaces in the  $\mathbb{E}(\kappa, \tau)$  spaces.** As stated in Definition 1.2 in the Introduction, given  $\mathfrak{h} \in C^1([-1, 1])$  an  $\mathfrak{h}$ -surface in an  $\mathbb{E}(\kappa, \tau)$  space is an immersed surface  $\Sigma$  whose mean

curvature satisfies  $H_\Sigma(p) = \mathfrak{h}(\nu_p)$ , for every  $p \in \Sigma$ . For short, we will say that  $\Sigma$  is an  $\mathfrak{h}$ -surface.

Next we describe the isometries in the  $\mathbb{E}(\kappa, \tau)$  spaces that are induced as isometries for the class of immersed  $\mathfrak{h}$ -surfaces. As a matter of fact, from Equation (1.1) we see that:

- Every isometry in  $\mathbb{E}(\kappa, \tau)$  that leaves invariant the angle function is also an isometry for  $\mathfrak{h}$ -surfaces.
- If an isometry changes the value of the angle function, and  $\mathfrak{h}$  is invariant under this symmetry, then the isometry is also induced for  $\mathfrak{h}$ -surfaces.

For instance, translations and rotations around the fibers leave invariant the angle function at any  $\mathbb{E}(\kappa, \tau)$  space. Moreover, if  $\tau = 0$  then the reflection w.r.t. vertical planes also leave invariant the angle function. Hence, these isometries are induced as isometries for the class of  $\mathfrak{h}$ -surfaces immediately.

The only isometries in the  $\mathbb{E}(\kappa, \tau)$  spaces that change the value of  $\nu$  are reflections with respect to horizontal planes if  $\tau = 0$ , and rotations of angle  $\pi$  around horizontal geodesics if  $\tau \neq 0$ ; any of these isometries change the value  $\nu$  into  $-\nu$ . Hence, if  $\mathfrak{h}$  is an even function,  $\Sigma$  is an  $\mathfrak{h}$ -surface,  $p \in \Sigma$  and  $\Psi$  is any of those isometries, we have

$$H_{\Psi(\Sigma)}(\Psi(p)) = H_\Sigma(p) = \mathfrak{h}(\nu_p) = \mathfrak{h}(-\nu_p) = \mathfrak{h}(\tilde{\nu}_{\Psi(p)})$$

where  $\tilde{\nu}$  is the angle function of  $\Psi(\Sigma)$ . In conclusion,  $\Psi(\Sigma)$  is also an  $\mathfrak{h}$ -surface and so  $\Psi$  is an isometry for  $\mathfrak{h}$ -surfaces.

**2.3 Existence of radial solutions.** In this section we show the existence of radial solutions for graphical  $\mathfrak{h}$ -surfaces defined over a disk with small enough radius. These examples will be of importance throughout our study of rotational  $\mathfrak{h}$ -surfaces.

First, we introduce some notation. We will define the *origin* of  $\mathbb{M}^2(\kappa)$  and denote it by  $\mathbf{o}$ , as the point  $\pi((0, 0, 0))$ , where  $(0, 0, 0)$  is the origin in the model  $\mathcal{R}(\kappa, \tau)$ . For example, if  $\kappa < 0$  the origin  $\mathbf{o}$  is just the origin of the Euclidean disk  $\mathbb{D}(0, 2/\sqrt{-\kappa})$ ; if  $\kappa = 0$  then  $\mathbf{o}$  is the origin of  $\mathbb{R}^2$ ; and if  $\kappa > 0$  and the section  $\{z = 0\}$  is identified with  $\mathbb{S}^2(\kappa) - \{q\}$ , then  $\mathbf{o}$  is the antipodal point  $-q$ .

The following proposition is consequence of a more general existence result for radial solutions of a fully non-linear PDE in the  $\mathbb{E}(\kappa, \tau)$  spaces, see Lemma 4.1 in [GaMi3].

**Proposition 2.1** *Let be  $\mathfrak{h} \in C^1([-1, 1])$ . There exists  $\delta > 0$  and a function  $f : [0, \delta] \rightarrow \mathbb{R}$  such that the radial graph over the distance disk  $D(\mathbf{o}, \delta)$  in  $\mathbb{M}^2(\kappa)$ ,*

$$\Sigma_f := \{(x \cos \theta, x \sin \theta, f(x)); x \in [0, \delta], \theta \in [0, 2\pi]\}, \quad f'(0) = 0,$$

*with upwards orientation is an  $\mathfrak{h}$ -surface in  $\mathcal{R}(\kappa, \tau)$ . Moreover,  $\Sigma_f$  is unique among graphical  $\mathfrak{h}$ -surfaces over  $D(\mathbf{o}, \delta)$  having constant boundary data.*

*The same holds for downwards orientation.*

### 3 Rotational $\mathfrak{h}$ -surfaces in homogeneous 3-spaces

**3.1. Basic formulas.** We begin by locally parametrizing a rotational  $\mathfrak{h}$ -surface in the coordinate model  $\mathcal{R}(\kappa, \tau)$ . Let  $\alpha(u) = (x(u), 0, z(u))$  be a curve in the  $xz$ -plane<sup>2</sup>. The map

$$\psi(u, \theta) = (x(u) \cos \theta, x(u) \sin \theta, z(u)),$$

defines an immersed surface  $\Sigma$  as the image of  $\alpha(u)$  under the rotations of  $\mathcal{R}(\kappa, \tau)$  that leave the  $E_3$ -axis pointwise fixed. Note that the projection  $\pi(\psi(u, \theta))$  lies in the section  $\{z = 0\} \subset \mathcal{R}(\kappa, \tau)$ . For  $\kappa \geq 0$  this reads as  $x(u) \in (0, \infty)$  (since the section  $\{z = 0\}$  is  $\mathbb{R}^2$ ), but for  $\kappa < 0$  this implies that  $x(u) \in (0, 2/\sqrt{-\kappa})$ .

The angle function of  $\Sigma$  in this model is

$$\nu = \frac{4x'}{\sqrt{16(1 + \tau^2 x^2)x'^2 + z'^2(4 + \kappa x^2)^2}},$$

and the mean curvature  $H_\Sigma$  has the following expression

$$2H_\Sigma = \frac{(4 + \kappa x^2)^2 (z'^3 (16 - \kappa^2 x^4) - 16z' (\tau^2 x^3 x'' + x x'' - x'^2) + 16z'' x x' (1 + \tau^2 x^2))}{4x (z'^2 (4 + \kappa x^2)^2 + 16x'^2 (1 + \tau^2 x^2))^{3/2}}. \quad (3.1)$$

Now we consider the metric

$$d\sigma^2 = (1 + \tau^2 x^2)dx^2 + \frac{(4 + \kappa x^2)^2}{16}dz^2 \quad (3.2)$$

in the  $xz$ -plane and the arc-length parameter  $s$  of  $\alpha$  with respect to this metric. A straightforward computation shows that, with this arc-length parameter, the angle function is  $\nu = x'$  and the mean curvature is

$$2\varepsilon H_\Sigma = \frac{x(-x''(4 + \kappa x^2)(1 + \tau^2 x^2) + x x'^2(\kappa - 8\tau^2) - \kappa x) - 4x'^2 + 4}{4x\sqrt{1 - x'^2(1 + \tau^2 x^2)}}, \quad \varepsilon := \text{sign}(z'). \quad (3.3)$$

From now on we suppose that  $\Sigma$  is an  $\mathfrak{h}$ -surface for some  $\mathfrak{h} \in C^1([-1, 1])$ , that is  $H_\Sigma(p) = \mathfrak{h}(\nu_p)$ ,  $\forall p \in \Sigma$ . Solving Equation (3.3) for  $x''$  yields

$$x'' = \frac{4 - \kappa x^2 - x'^2(4 - x^2(\kappa - 8\tau^2)) - 8\varepsilon x \mathfrak{h}(x')\sqrt{1 - (1 + \tau^2 x^2)x'^2}}{x(4 + \kappa x^2)(1 + \tau^2 x^2)}.$$

After the change of variable  $x' = y$ , this equation transforms into the first order, autonomous system

$$\begin{pmatrix} x \\ y \end{pmatrix}' = \begin{pmatrix} y \\ \frac{4 - \kappa x^2 - y^2(4 - x^2(\kappa - 8\tau^2)) - 8\varepsilon x \mathfrak{h}(y)\sqrt{1 - (1 + \tau^2 x^2)y^2}}{x(4 + \kappa x^2)(1 + \tau^2 x^2)} \end{pmatrix}. \quad (3.4)$$

<sup>2</sup>The  $xz$ -plane is just the subset  $\{y = 0\}$  in  $\mathcal{R}(\kappa, \tau)$ . Only when  $\tau = 0$  it is a totally geodesic surface in  $\mathbb{E}(\kappa, \tau)$  isometric to  $\mathbb{R}^2$ .



From the arc-length condition  $(1 + \tau^2 x^2)x'^2 + (4 + \kappa x^2)^2/16z'^2 = 1$  we have that the angle function  $x'$  satisfies

$$\frac{-1}{1 + \tau^2 x^2} \leq \nu \leq \frac{1}{1 + \tau^2 x^2},$$

with equality if and only if the height function  $z$  of  $\alpha$  has a local extremum. This implies that system (3.4) is only defined for points  $(x_0, y_0)$  such that  $x_0 > 0$  and  $y_0^2 \leq 1/(1 + \tau^2 x_0^2)$ . For instance, note that for the case  $\tau > 0$ , the angle function satisfies  $\nu = \pm 1$  if and only if  $x = 0$ , which only happens at the axis of rotation.

**3.2. The phase plane.** The phase plane of Equation (3.4) is defined as the set

$$\Theta_\varepsilon := \left\{ (x, y); x > 0 \text{ and } y^2 < \frac{1}{1 + \tau^2 x^2} \right\},$$

with coordinates  $(x, y)$  denoting the distance to the axis of rotation and the angle function. Note that if  $\kappa < 0$ , then the  $x$ -coordinate is defined for  $0 < x < 2/\sqrt{-\kappa}$  and if  $\kappa \geq 0$ , the  $x$ -coordinate is defined for every  $x > 0$ .

The boundary of  $\Theta_\varepsilon$  consists of the segment  $\{0\} \times [-1, 1]$  and the vertical graphs  $y = \pm 1/\sqrt{1 + \tau^2 x^2}$ . We will denote by  $\Omega^+$  (resp.  $\Omega^-$ ) to the component  $y = 1/\sqrt{1 + \tau^2 x^2}$  (resp. to the component  $y = -1/\sqrt{1 + \tau^2 x^2}$ ), and by  $\Omega := \Omega^+ \cup \Omega^-$ . For instance, if  $\tau = 0$  then  $\Omega$  consists of the parallel lines  $\{y = \pm 1\}$ , and if  $\tau > 0$  then  $\Omega$  consists of two curves having the points  $(0, \pm 1)$  as endpoints.

The orbits are the solutions of system (3.4) and will be denoted by  $\gamma(s) = (x(s), y(s))$ . The existence and uniqueness of the Cauchy problem associated to Equation (3.4) has as consequence two important facts: *i*) two different orbits cannot intersect in  $\Theta_\varepsilon$ , and *ii*) the orbits are a foliation of  $\Theta_\varepsilon$  by regular, proper  $C^1$  curves.

Although we will remind it in the statement of the main results, **hereinafter  $\mathfrak{h}$  will be always supposed to lie in the space  $\mathfrak{C}^1$** , see Equation (1.2) for a definition of the space  $\mathfrak{C}^1$ .

For example, the fact that  $\mathfrak{h}$  is even has the following consequence on the phase plane  $\Theta_\varepsilon$ : if  $\gamma(s) = (x(s), y(s))$  is a solution to Equation (3.4), so it is  $\tilde{\gamma}(s) = (x(-s), -y(-s))$ . Geometrically, this means that any orbit in the phase plane  $\Theta_\varepsilon$  is symmetric with respect to the axis  $y = 0$ . This condition is related with the fact that horizontal reflections for  $\tau = 0$  and rotations of angle  $\pi$  around horizontal geodesics if  $\tau > 0$ , are isometries for  $\mathfrak{h}$ -surfaces.

Since  $\mathfrak{h} \in \mathfrak{C}^1$ , a trivial solution to system (3.4) in  $\Theta_1$  is the one given by the constant orbit

$$x(s) = \frac{2}{\sqrt{4\mathfrak{h}(0)^2 + \kappa + 2\mathfrak{h}(0)}}, \quad y(s) = 0. \quad (3.5)$$

This point is the *equilibrium* of (3.4) and will be denoted by  $e_0$ . This equilibrium generates an  $\mathfrak{h}$ -surface with constant distance to the axis of rotation and with vanishing angle function, that is, a vertical, circular cylinder<sup>3</sup> with constant mean curvature equal to  $\mathfrak{h}(0)$ .

<sup>3</sup>In  $\mathbb{S}_b^3(\kappa, \tau)$ , this cylinder is identified as a compact torus which is the inverse image of a circle in  $\mathbb{S}^2$  by the Hopf fibration. These CMC tori were called *Hopf tori* in [Tor].

Note that for  $\kappa > 0$ , i.e. in  $\mathbb{S}^2(\kappa) \times \mathbb{R}$  and  $\mathbb{S}_b^3(\kappa, \tau)$ , the orbit in  $\Theta_{-1}$  defined by

$$x(s) = \frac{2}{\sqrt{4\mathfrak{h}(0)^2 + \kappa - 2\mathfrak{h}(0)}}, \quad y(s) = 0, \quad (3.6)$$

is also a solution of Equation (3.4) for  $\varepsilon = -1$ . This point will be called the *equilibrium* of  $\Theta_{-1}$  and denoted by  $e_{-1}$ . Again, the  $\mathfrak{h}$ -surface generated by  $e_{-1}$  is a vertical CMC cylinder in  $\mathbb{S}^2(\kappa) \times \mathbb{R}$  or a Hopf torus in  $\mathbb{S}_b^3(\kappa, \tau)$ ; see Section 4 and Figure 3. In the next section, we will see that no equilibria exist in  $\Theta_{-1}$  for  $\kappa \leq 0$ .

From Equation (3.4) we see that the points in  $\Theta_\varepsilon$  with  $y'(s) = 0$  are the ones lying in the intersection of  $\Theta_\varepsilon$  with the (possibly disconnected) horizontal graph:

$$x = \Gamma_\varepsilon(y) := 2\sqrt{\frac{1 - y^2}{\kappa(1 - y^2) + 8(\mathfrak{h}(y)^2 + \tau^2 y^2) + 4\varepsilon\mathfrak{h}(y)\sqrt{4\mathfrak{h}(y)^2 + \kappa(1 - y^2) + 4\tau^2 y^2}}}. \quad (3.7)$$

We define  $\Gamma_\varepsilon := \{x = \Gamma_\varepsilon(y)\} \cap \Theta_\varepsilon$ . Note that the points lying in  $\Gamma_\varepsilon$  correspond to points whose angle function has vanishing derivative, and that  $\Gamma_1 \cap \{y = 0\} = e_0$  and  $\Gamma_{-1} \cap \{y = 0\} = e_{-1}$  for  $\kappa > 0$ . Again, since  $\mathfrak{h}$  is even we get that  $\Gamma_\varepsilon$  is symmetric with respect to the axis  $y = 0$ .

**Observation 3.1** *We must clarify the difference between existing an equilibrium point in  $\Theta_{-1}$  and the point given by  $(\Gamma_{-1}(0), 0)$ . Even though the latter can exist (for the case that  $\Gamma_{-1}(0)$  is well defined), the point  $(\Gamma_{-1}(0), 0)$  may not lie in  $\Theta_{-1}$ . For instance, if  $\kappa < 0$  we will see that  $\Gamma_{-1}(0) > 2/\sqrt{-\kappa}$ , hence it lies outside  $\Theta_{-1}$ . The case  $\kappa = 0$  can be seen as a limit when  $\kappa < 0$  tends to zero; in fact, for  $\kappa = 0$  it can be easily seen that  $\Gamma_{-1}(0)$  is not defined.*

**3.3. The behavior of  $\Gamma_\varepsilon$ .** As revealed in the study made in  $\mathbb{R}^{n+1}$  in [BGM1], the curve  $\Gamma_\varepsilon$  deeply governs the behavior of the orbits in  $\Theta_\varepsilon$ . We study next the properties of the curve  $\Gamma_\varepsilon$  in the different phase planes.

First, recall that the range of the  $x$ -coordinate in  $\Theta_\varepsilon$  depends on the value of  $\kappa$ . For the case that  $\kappa \geq 0$ , the phase plane  $\Theta_\varepsilon$  is defined for every  $x > 0$ . For  $\kappa < 0$ ,  $\Theta_\varepsilon$  is defined for  $0 < x < 2/\sqrt{-\kappa}$ . Because of the restrictions on  $x$  for  $\kappa < 0$ , the curve  $\Gamma_\varepsilon$  can leave  $\Theta_\varepsilon$ , or even not exist. Nonetheless, we will see that  $\Gamma_1$  is always contained in  $\Theta_1$ .

**Claim 1.** The curve  $\Gamma_1$  for  $\kappa < 0$  lies entirely in  $\Theta_1$ , i.e.  $\Gamma_1(y) < 2/\sqrt{-\kappa}$ ,  $\forall y \in [-1, 1]$ .

*Proof of the claim :* From (3.7) we see that  $\Gamma_1(y) < 2/\sqrt{-\kappa}$  if and only if

$$-\kappa(1 - y^2) < \kappa(1 - y^2) + 8(\mathfrak{h}(y)^2 + \tau^2 y^2) + 4\mathfrak{h}(y)\sqrt{4\mathfrak{h}(y)^2 + \kappa(1 - y^2) + 4\tau^2 y^2}.$$

Simplifying we arrive to

$$0 < 4\mathfrak{h}(y)^2 + \kappa(1 - y^2) + 4\tau^2 y^2 + 2\mathfrak{h}(y)\sqrt{4\mathfrak{h}(y)^2 + \kappa(1 - y^2) + 4\tau^2 y^2}.$$

Since  $\mathfrak{h} \in \mathcal{C}^1$  in particular  $4\mathfrak{h}(y)^2 + \kappa(1 - y^2) > 0$  holds for every  $y \in [-1, 1]$ , hence the above inequality yields.  $\square$

In any case, the curve  $\Gamma_1$  is a connected, compact arc in  $\Theta_1$  and having the points  $(0, \pm 1)$  as endpoints. With the same ideas it is straightforward to check that for  $\kappa > 0$ , the equilibrium  $e_0 = \Gamma_1 \cap \{y = 0\}$  is at the left-hand side of the point  $(2/\sqrt{\kappa}, 0)$ .

Now, we focus on the curve  $\Gamma_{-1}$  in the different spaces. The proof of the following claim holds immediately by just substituting in Equation (3.7) the value  $\kappa = 0$ .

**Claim 2.** If  $\kappa = 0$  and  $\tau > 0$  (i.e. in the Heisenberg space) the curve  $\Gamma_{-1}$  is a disconnected bi-graph over the axis  $y = 0$ , having the points  $(0, \pm 1)$  as endpoints and an asymptote at  $y = 0$ .

As we pointed out, for  $\kappa < 0$  the curve  $\Gamma_{-1}$  may leave the phase plane  $\Theta_{-1}$ . The following claim reveals that the point  $(\Gamma_{-1}(0), 0)$  is well defined, and lies outside  $\Theta_{-1}$ .

**Claim 3.** If  $\kappa < 0$ , then the value  $\Gamma_{-1}(0)$  is well defined and  $\Gamma_{-1}(0) > 2/\sqrt{-\kappa}$ .

*Proof of the claim :* Substituting  $\Gamma_{-1}(0)$  in Equation (3.7) and simplifying, we get

$$\Gamma_{-1}(0) = \frac{2}{2\mathfrak{h}(0) - \sqrt{4\mathfrak{h}(0)^2 + \kappa}}.$$

Since  $\kappa < 0$ , the denominator in the above fraction is always well-defined and so it is the value  $\Gamma_{-1}(0)$ .

For proving that  $\Gamma_{-1}(0) > 2/\sqrt{-\kappa}$ , after a similar computation as in Claim 1. we get

$$0 > 4\mathfrak{h}(0)^2 + \kappa - 2\mathfrak{h}(0)\sqrt{4\mathfrak{h}(0)^2 + \kappa} = \sqrt{4\mathfrak{h}(0)^2 + \kappa} \left( \sqrt{4\mathfrak{h}(0)^2 + \kappa} - 2\mathfrak{h}(0) \right).$$

This time, since  $\kappa < 0$  we have that the latter expression is negative, concluding the proof.  $\square$

By the previous claim, for  $\kappa < 0$  and  $\tau > 0$  the curve  $\Gamma_{-1}$  has the point  $(0, \pm 1)$  as endpoints, and then *leaves*  $\Theta_{-1}$  before intersecting the axis  $y = 0$ . In particular,  $\Gamma_{-1}$  is disconnected and no equilibria exist in  $\Theta_{-1}$  when  $\kappa \leq 0$ .

When  $\tau > 0$ , i.e. in the Berger spheres  $\mathbb{S}_b^3(\kappa, \tau)$ , we have the following configuration for  $\Gamma_{-1}$ :

**Claim 4.** If  $\kappa > 0, \tau > 0$ , then  $\Gamma_{-1}(0) > 2/\sqrt{\kappa}$  and  $\Gamma_{-1}(\pm 1) = 0$ .

*Proof of the claim :* The fact that  $\Gamma_{-1}(0) > 2/\sqrt{\kappa}$  is equivalent to:

$$\sqrt{4\mathfrak{h}(0)^2 + \kappa} > 2\mathfrak{h}(0),$$

which obviously holds since  $\kappa > 0$ .

Now,  $\Gamma_{-1}(\pm 1) = 0$  is trivial by just substituting; the numerator vanishes and the denominator equals

$$\sqrt{\mathfrak{h}(\pm 1)^2 + \tau^2} \left( \sqrt{\mathfrak{h}(\pm 1)^2 + \tau^2} - \mathfrak{h}(\pm 1) \right),$$

which again is positive since  $\tau > 0$ . Hence,  $\Gamma_{-1}$  is a compact arc in  $\Theta_{-1}$  joining the points  $(0, 1)$  and  $(0, -1)$ .  $\square$

Next, we focus on the product spaces. The following claim proves that for the case  $\kappa < 0$  and  $\tau = 0$  corresponding to the space  $\mathbb{H}^2(\kappa) \times \mathbb{R}$ , the curve  $\Gamma_{-1}$  does not even appear in  $\Theta_{-1}$ . In other words:

**Claim 5.** If  $\kappa < 0$ ,  $\tau = 0$ , then  $\Gamma_{-1}(y) > 2/\sqrt{-\kappa}$ ,  $\forall y \in [-1, 1]$ .

*Proof of the claim :* Arguing as in Claim 2, the fact that  $\Gamma_{-1}(y) > 2/\sqrt{-\kappa}$  holds is equivalent to the following inequality, this time for every  $y \in [-1, 1]$ .

$$0 > \sqrt{4\mathfrak{h}(y)^2 + \kappa(1 - y^2)} \left( \sqrt{4\mathfrak{h}(y)^2 + \kappa(1 - y^2)} - 2\mathfrak{h}(y) \right).$$

Again, the fact that  $\kappa < 0$  makes true this inequality for every  $y \in (-1, 1)$ . At  $y = \pm 1$  the curve  $\Gamma_{-1}$  tends to infinity, concluding the proof.  $\square$

Finally, we describe  $\Gamma_{-1}$  for the case that  $\kappa > 0$ . When  $\tau = 0$ , i.e. in the space  $\mathbb{S}^2(\kappa) \times \mathbb{R}$ , we have the following:

**Claim 6.** If  $\kappa > 0$ ,  $\tau = 0$ , then  $\Gamma_{-1}(y) > 2/\sqrt{\kappa}$ ,  $\forall y \in [-1, 1]$ .

*Proof of the claim :* As in the previous claims, the desired inequality is equivalent to the following one

$$\mathfrak{h}(y)\sqrt{4\mathfrak{h}(y)^2 + \kappa(1 - y^2)} > 2\mathfrak{h}(y)^2.$$

After simplification we get

$$\kappa(1 - y^2) > 0,$$

which holds at every value  $y \in (-1, 1)$ . At the values  $y = \pm 1$  the curve  $\Gamma_{-1}$  tends to infinity, hence the claim is proved.  $\square$

In any of the cases, depending on the different values of  $\kappa, \tau$  and  $\varepsilon = \pm 1$ , the curve  $\Gamma_\varepsilon$  and the axis  $y = 0$  divide  $\Theta_\varepsilon$  into connected components, which we will call *monotonicity regions*, where the coordinates  $(x(s), y(s))$  of any orbit are monotonous functions. Hence the behavior of an orbit is uniquely determined by the monotonicity region where it belongs. We describe this behavior next.

**Proposition 3.2** *Let be  $(x_0, y_0) \in \Theta_\varepsilon$  and consider an orbit  $\gamma(s) = (x(s), y(s))$  such that  $\gamma(s_0) = (x_0, y_0)$ . Then, the following properties hold:*

1. *If  $y_0 = 0$ , then  $\gamma$  is orthogonal to the axis  $y = 0$ . If  $y_0 \neq 0$ , then we can see  $\gamma(s)$  locally around  $\gamma(s_0)$  as a graph  $y(x)$ . Then:*
2. *If  $x_0 > \Gamma_\varepsilon(y_0)$  (resp.  $x_0 < \Gamma_\varepsilon(y_0)$ ) and  $y_0 > 0$ , then  $y(x)$  is strictly decreasing (resp. increasing) at  $x_0$ .*
3. *If  $x_0 > \Gamma_\varepsilon(y_0)$  (resp.  $x_0 < \Gamma_\varepsilon(y_0)$ ) and  $y_0 < 0$ , then  $y(x)$  is strictly increasing (resp. decreasing) at  $x_0$ .*
4. *If  $x_0 = \Gamma_\varepsilon(y_0)$ , then  $y'(x_0) = 0$  and  $y(x)$  has a local extremum at  $x_0$ .*

*Proof:* First, we study how an orbit intersects the axis  $y = 0$ . Suppose that  $\varepsilon = 1$  and let  $\gamma(s) = (x(s), y(s))$  be an orbit in  $\Theta_1$  such that  $\gamma(0) = (x_0, 0)$  for  $x_0 > 0$ . Moreover, suppose that  $(x_0, 0)$  is not the equilibrium point. From Equation (3.4) we get

$$\gamma'(0) = \left( 0, \frac{4 - x_0(8\mathfrak{h}(0) + \kappa x_0)}{x_0(4 + \kappa x_0^2)(1 + \tau^2 x_0^2)} \right).$$

So,  $\gamma'(0)$  intersects orthogonally  $y = 0$ , and it does either upwards or downwards depending on the sign of  $p_\kappa(x_0)$ , where  $p_\kappa(x) = 4 - x(8\mathfrak{h}(0) + \kappa x)$ . Note that if  $\kappa \neq 0$ , the zeroes of  $p_\kappa(x)$  are

$$x_\pm = \frac{2}{2\mathfrak{h}(0) \pm \sqrt{4\mathfrak{h}(0)^2 + \kappa}},$$

and the point  $(x_+, 0) \in \Theta_1$  agrees with the equilibrium  $e_0$  defined in (3.5). Depending on the values of  $\kappa$ , this parabola behaves as follows (see Figure 1):

- For  $\kappa > 0$ ,  $x_- < 0$  and  $x_+ > 0$ , and  $p_\kappa(x) > 0$  for  $x \in (0, x_+)$ .
- For  $\kappa = 0$ ,  $p_\kappa(x)$  reduces to the straight line  $y(x) = 4 - 8\mathfrak{h}(0)x$ , which has the point  $x_+ = 1/(2\mathfrak{h}(0))$  as zero.
- For  $\kappa < 0$ ,  $x_-, x_+ > 0$ ,  $x_+ < x_-$ , and  $p_\kappa(x) > 0$  for  $x \in (0, x_+)$ . Moreover,  $x_+ < 2/\sqrt{-\kappa} < x_-$ .

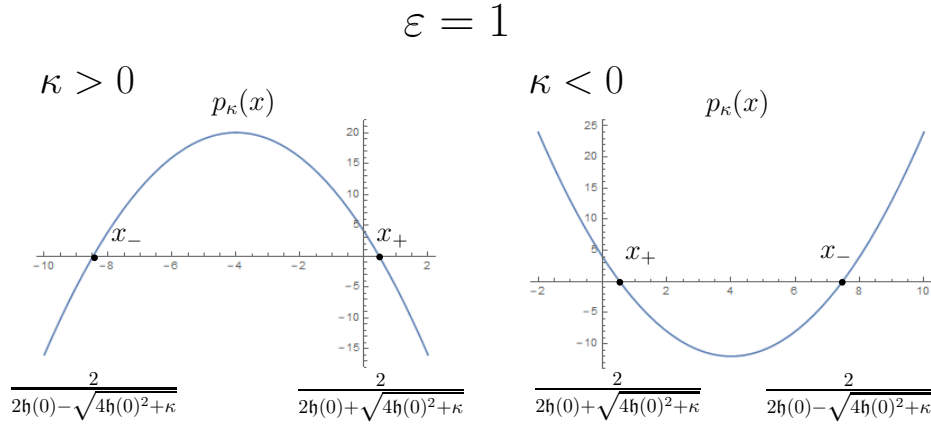


Figure 1: The parabola  $p_\kappa(x)$  and its zeroes, depending if  $\kappa > 0$  or  $\kappa < 0$ .

Now, we go back to the study of  $\gamma'(0)$ . First, suppose that  $(x_0, 0)$  lies at the left hand side of  $e_0$ , i.e.  $x_0 < x_+$ . Hence,  $p_\kappa(x_0) > 0$  and thus  $\gamma'(0)$  intersects orthogonally the axis  $y = 0$  pointing upwards. Analogously,  $\gamma'(0)$  points downward whenever  $(x_0, 0)$  lies at the right-hand side of  $e_0$ , i.e. when  $x_0 > x_+$ .

In  $\Theta_{-1}$  the situation is similar. Again, let  $\gamma(s)$  be an orbit in  $\Theta_{-1}$  such that  $\gamma(0) = (x_0, 0)$  for  $x_0 > 0$ . This time, the value  $\gamma'(0)$  is given by

$$\gamma'(0) = \left( 0, \frac{4 + x_0(8\mathfrak{h}(0) - \kappa x_0)}{x_0(4 + \kappa x_0^2)(1 + \tau^2 x_0^2)} \right),$$

hence its behavior is determined by the parabola  $q_\kappa(x) = 4 + x(8\mathfrak{h}(0) - \kappa x)$ . Now, if  $\kappa \neq 0$ ,  $q_\kappa(x)$  has as zeros  $z_\pm = -x_\pm$ , where  $x_\pm$  are the zeroes of  $p_\kappa(x)$ . Recall that for  $\kappa > 0$  we have the existence of the equilibrium in  $\Theta_{-1}$ , this time given by  $e_{-1} = (z_-, 0)$ . Therefore,  $q_\kappa(x)$  behaves as follows:

- For  $\kappa > 0$ ,  $z_+ < 0$  and  $z_- > 0$ ,  $q_\kappa(x) > 0$  for  $x \in (0, z_-)$  and  $q_\kappa(x) < 0$  for  $x > z_-$ .
- For  $\kappa = 0$ ,  $q_\kappa(x)$  reduces to the straight line  $y(x) = 4 + 8\mathfrak{h}(0)x$ , which has the point  $x = -1/(2\mathfrak{h}(0))$  as zero. In particular,  $q_\kappa(x) > 0$ ,  $\forall x > 0$ .
- For  $\kappa < 0$ ,  $z_-, z_+ < 0$ , and  $q_\kappa(x) > 0$  for every  $x > 0$ .

In conclusion, if  $\kappa \leq 0$  then  $\gamma'(0)$  points upwards at every  $(x_0, 0) \in \Theta_{-1}$ . If  $\kappa > 0$  then  $\gamma'(0)$  points upwards at  $(x_0, 0)$  if  $x_0 < z_-$ , and downwards if  $x_0 > z_-$ .

We have the following consequence in  $\Theta_1$ : let  $(x_0, 0)$  be a point at the left-hand side of  $e_0$ , and choose  $r > 0$  such that  $D((x_0, 0), r) \cap \Gamma_1 = \emptyset$ . Let  $\gamma(s)$  be an orbit in  $D((x_0, 0), r)$  such that  $\gamma(0) = (x_0, 0)$ . Then, the sign of  $y'(s)$  is constant and equal to the sign of  $y'(0)$ , which is positive. By connectedness, the sign of  $y'(s)$  of any orbit in  $\Lambda_3 \cup \Lambda_4$  is also positive. The same holds for an orbit contained in  $\Lambda_1^+ \cup \Lambda_2^+$ , but this time  $y'(s)$  is negative.

A similar situation holds in  $\Theta_{-1}$  in the monotonicity regions  $\Lambda^+$  and  $\Lambda^-$  if  $\tau = 0$ , and  $\Lambda_3^-$  and  $\Lambda_4^-$  if  $\tau > 0$ ; we have  $y'(s) > 0$  for any orbit contained in those regions. Finally, we prove that  $y'(s) < 0$  for an orbit contained in  $\Lambda_1^-$  or  $\Lambda_2^-$  in  $\Theta_{-1}$  if  $\tau > 0$ .

The continuity argument aforementioned can be only done when  $\kappa > 0$ , i.e. in the spaces  $\mathbb{S}^2 \times \mathbb{R}$  and  $\mathbb{S}_b^3(\kappa, \tau)$ , since in these cases  $\Theta_{-1}$  has an equilibrium  $e_{-1}$  and we can compare  $\gamma'(0)$  at the left and right-hand side of  $e_{-1}$ . By symmetry of the phase plane w.r.t. the axis  $y = 0$  it only suffices to prove it in the region  $\Lambda_1^-$ . Fix a point  $(x_\infty, y_\infty) \in \Omega^+$  and let  $\gamma(s_n) = (x(s_n), y(s_n)) = (x_n, y_n)$  be a sequence of points in an orbit  $\gamma(s)$  lying in  $\Lambda_1^-$  and converging to  $(x_\infty, y_\infty)$ . Note that  $(x_\infty, y_\infty)$  are both positive. From Equation (3.4) we see that the values  $\gamma'(s_n)$  satisfy:

$$\begin{pmatrix} x'(s_n) \\ y'(s_n) \end{pmatrix} = \begin{pmatrix} y_n \\ \frac{4 - \kappa x_n^2 - y_n^2(4 - x_n^2(\kappa - 8\tau^2)) + 8x_n\mathfrak{h}(y_n)\sqrt{1 - (1 + \tau^2 x_n^2)y_n^2}}{x_n(4 + \kappa x_n^2)(1 + \tau^2 x_n^2)} \end{pmatrix}.$$

Since  $(x_\infty, y_\infty) \in \Omega^+$  we get  $y_\infty^2(1 + \tau^2 x_\infty^2) = 1$ . Taking limits we see that the value  $y'(s_n)$  converge to  $-(1 - y_\infty^2)(4 + \kappa x_\infty^2)$ , which is negative. Because  $y'(s) = 0$  only happens at  $\Gamma_{-1}$ , by continuity we get  $y'(s) < 0$ . Again, a connectedness argument ensures us that this condition is fulfilled for every orbit lying in  $\Lambda_1^-$ , and by symmetry also in  $\Lambda_2^-$ .

This completes the proof of Proposition 3.2.  $\square$

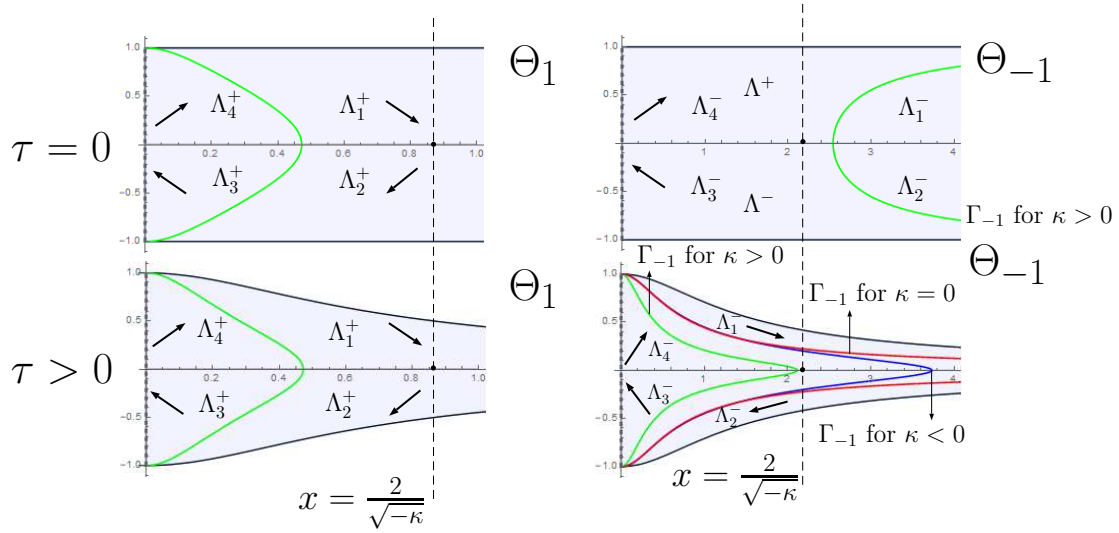


Figure 2: The phase plane  $\Theta_\varepsilon$ , the curve  $\Gamma_\varepsilon$  for the different values of  $\kappa$  and  $\tau$ , and the monotonicity regions.

**3.4. The structure of the phase plane.** In the previous section we focused in how the orbits behave in each monotonicity region, hence how they move through  $\Theta_\varepsilon$ . In this section we exhibit further properties of the phase plane that determine the global and local behavior of an orbit  $\gamma(s)$  as it approaches to some point, or tends to *escape* from  $\Theta_\varepsilon$ . These properties are strongly influenced by the underlying geometric problem.

We point out that since  $e_0$  is a solution of Equation (3.4), because  $\mathfrak{h} \in C^1$  and by uniqueness of the Cauchy problem, an orbit could converge to  $e_0$  with the parameter  $s \rightarrow \infty$ . In fact, in [BGM1] we constructed explicit examples converging *directly* to  $e_0$ , that is without spiraling around it. However, this situation cannot happen if  $\mathfrak{h}$  is even, as detailed next.

**Proposition 3.3** *An orbit  $\gamma$  in  $\Theta_1$  cannot converge to  $e_0$  or  $e_{-1}$  (for  $\kappa > 0$ ).*

*Proof:* Let us analyze the structure of the orbits around  $e_0$ . The fact that  $\mathfrak{h}$  is even implies that  $\mathfrak{h}'(0) = 0$ , and the linearized system of Equation (3.4) at  $e_0$  is

$$\begin{pmatrix} u \\ v \end{pmatrix}' = \begin{pmatrix} 0 & 1 \\ F(\kappa, \tau, \mathfrak{h}(0)) & 0 \end{pmatrix} \begin{pmatrix} u \\ v \end{pmatrix},$$

where  $F(\kappa, \tau, \mathfrak{h}(0))$  is a negative expression only depending on the mentioned variables; the fact that  $\mathfrak{h} \in \mathfrak{C}^1$  is key here and in how the element  $a_{22}$  in the linearized matrix vanishes.

Hence, the orbits of the linearized system around the origin are ellipses, and by classical theory of non-linear autonomous systems we have two possible configurations around  $e_0$ : either the curves are closed, or they spiral around  $e_0$ , converging to it. However, the latter possibility cannot occur since the phase plane  $\Theta_1$  is symmetric with respect to  $y = 0$ , and  $e_0$  belongs to this axis. In particular, all the orbits in  $\Theta_1$  stays at a positive distance from  $e_0$ .

This proof carries over verbatim for the equilibrium point  $e_{-1}$  of the phase plane  $\Theta_{-1}$  when  $\kappa > 0$ .  $\square$

Next, we analyze the boundary points of  $\Theta_\varepsilon$  that cannot be limit points of orbits.

**Proposition 3.4** *An orbit  $\gamma$  cannot converge to a point  $(0, y) \in \overline{\Theta_\varepsilon}$ ,  $|y| < 1$ .*

*Proof:* By contradiction, suppose that such an orbit exists and let  $\alpha(s) = (x(s), 0, z(s))$  be its associated profile curve. Then,  $\gamma(s_n) \rightarrow (0, y)$ ,  $y \in (-1, 1)$ , for a sequence  $s_n$ . This implies that  $x(s_n) \rightarrow 0$  and  $x'(s_n) \rightarrow y \in (-1, 1)$ , that is  $\alpha(s)$  approaches to the  $E_3$ -axis in a non-orthogonal way.

Let  $\Sigma$  be the  $\mathfrak{h}$ -surface obtained by rotating  $\alpha$ . By the monotonicity properties of the phase plane, we see that a piece of  $\Sigma$  can be written as a graph  $z = u(x, y)$  over a punctured disk  $D(\mathbf{o}, \delta)$  in  $\mathbb{M}^2(\kappa)$ . Moreover, the mean curvature  $H(x, y)$  viewed as a function in  $D(\mathbf{o}, \delta) - \{\mathbf{o}\}$  extends continuously to  $\mathbf{o}$  with value  $\mathfrak{h}(y)$ . By the work of Leandro and Rosenberg [LeRo], we know that  $\Sigma$  extends smoothly to  $D$  having vertical unit normal at  $u(0, 0)$  and hence angle function equal to  $\pm 1$ . This contradicts the fact that  $|y| < 1$ .  $\square$

In particular, if an  $\mathfrak{h}$ -surface intersects the axis of rotation it does in an orthogonal way, i.e.  $x' = \pm 1$ . Also, Proposition 3.4 ensures us that an orbit  $\gamma(s)$  can only converge to points in the boundary of  $\Theta_\varepsilon$  located in  $\Omega$ . We ensure that  $\gamma(s)$  cannot converge to some  $(x_0, y_0) \in \Omega$  for the value of the parameter  $s \rightarrow \pm\infty$ . Indeed, if  $(x(s), y(s)) \rightarrow (x_0, y_0) \in \Omega$  for  $s \rightarrow \pm\infty$ , then the mean value theorem ensures us that  $x'(s) \rightarrow 0$ . But  $x'(s) = y(s) \rightarrow y_0 \neq 0$ , reaching to a contradiction. Hence, if  $\gamma(s)$  converges to  $\Omega$ , reaches it at a finite instant.

Recall that Equation (3.4) is singular for the Cauchy data  $x(0) = 0$ ,  $x'(0) = \pm 1$  missed by Proposition 3.4. However, in virtue of Proposition 2.1, we can construct radial  $\mathfrak{h}$ -surfaces intersecting orthogonally the axis of rotation over a small enough disk  $D(0, \delta)$ .

**Definition 3.5** *Let be  $\mathfrak{h} \in \mathcal{C}^1$ . We define the rotational  $\mathfrak{h}$ -surface  $\Sigma^+$  (resp.  $\Sigma^-$ ) as the upwards oriented (resp. downwards oriented) radial solution of Proposition 2.1.*

*Moreover,  $\Sigma^+$  and  $\Sigma^-$  agree after a vertical translation and a reflection with respect to a horizontal plane if  $\tau = 0$ , or a rotation around a horizontal geodesic if  $\tau > 0$ .*

The existence of  $\Sigma^+$  and  $\Sigma^-$  has the following implications on the phase plane  $\Theta_\varepsilon$ :

**Proposition 3.6** *There exists a unique orbit  $\gamma_+$  (resp.  $\gamma_-$ ) in  $\Theta_1$  having the point  $(0, 1)$  (resp.  $(0, -1)$ ) in  $\overline{\Theta_1}$  as endpoint. Moreover,  $\gamma_+$  and  $\gamma_-$  are symmetric with respect to the axis  $y = 0$ . There do not exist such orbits in  $\Theta_{-1}$ .*

*Proof:* If prove the existence of  $\gamma_+$ , the existence of  $\gamma_-$  follows from the symmetry of the phase plane  $\Theta_1$ .



In virtue of Lemma (2.1),  $\Sigma^+$  is described as the rotation of a curve  $\alpha(s) = (x(s), 0, z(s))$  around the  $E_3$ -axis and such that  $x(0) = 0$  and  $x'(0) = 1$ . Since the mean curvature of  $\Sigma^+$  at  $p_0$  is positive and  $\Sigma^+$  is upwards oriented, the mean curvature comparison principle yields  $z(s) > 0$  and  $z'(s) > 0$  for  $s > 0$  small enough. Thus, the orbit  $\gamma_+(s)$  generated by  $\alpha(s)$  belongs to  $\Theta_1$  for  $s > 0$  small enough.

The mean curvature comparison principle ensures us that such an orbit cannot exist in  $\Theta_{-1}$  for upwards oriented graphs. By symmetry of the phase plane we ensure that this condition also holds at the point  $(0, -1)$ , generating an orbit  $\gamma_-$  that corresponds to the  $\mathfrak{h}$ -surface  $\Sigma^-$ . Again,  $\gamma_-$  cannot exist in  $\Theta_{-1}$  by the mean curvature comparison principle.  $\square$

Thus, the orbit  $\gamma_+(s)$  starts at the point  $(0, 1) \in \overline{\Theta}_1$ , say at the instant  $s = 0$ , and then is strictly contained in the monotonicity region  $\Lambda_1^+$  for  $s > 0$  small enough. We ensure that  $\gamma_+(s)$  cannot intersect again the boundary component  $y = 1/\sqrt{1 + \tau^2 x^2}$ . In general, we prove that the orbits in  $\Theta_\varepsilon$  cannot have endpoints in  $\Omega$  arbitrarily.

**Proposition 3.7** *Let  $\gamma(s)$  be an orbit in  $\Theta_\varepsilon$  and consider  $\alpha(s) = (x(s), 0, z(s))$  the associated arc-length parametrized curve. Suppose that  $\gamma(s)$  has some  $(x_0, y_0) \in \Omega^\pm$  as endpoint at  $s = s_0$ . Then,*

1. *If  $\gamma(s_0) \in \Omega^+$ ,  $z(s)$  has a local minimum at  $s = s_0$ . In this case,  $\gamma(s)$  lies in  $\Theta_1$  for  $s > s_0$ . For  $s < s_0$ ,  $\gamma(s)$  belongs to  $\Theta_{-1}$ .*
2. *If  $\gamma(s_0) \in \Omega^-$ ,  $z(s)$  has a local maximum at  $s = s_0$ . In this case,  $\gamma(s)$  lies in  $\Theta_1$  for  $s < s_0$ . For  $s > s_0$ ,  $\gamma(s)$  belongs to  $\Theta_{-1}$ .*

*Proof:* Suppose that  $\gamma_+(s_0) = (x_0, y_0) \in \Omega^+$  for some  $s_0$  and let  $\alpha(s) = (x(s), 0, z(s))$  be the arc-length parametrized curve defined by  $\gamma(s)$ . Note that  $x'(s_0) = y_0 > 0$ . Because  $\gamma(s_0) \in \Omega^+$  we have that the angle function  $x'(s) = y(s)$  satisfies  $y(s_0) = 1/\sqrt{1 + \tau^2 x(s_0)^2}$ , and thus the arc-length condition

$$(1 + \tau^2 x(s)^2)x'(s)^2 + \frac{(4 + \kappa x(s)^2)^2}{16} z'(s)^2 = 1$$

ensures us that  $z'(s_0) = 0$ . From Equation (3.1) and the fact that  $z'(s_0) = 0$ , we get

$$2\mathfrak{h}(x'(s_0)) = \frac{(4 + \kappa x(s_0)^2)^2 16x'(s_0) (1 + \tau^2 x(s_0)^2)}{4(16x'(s_0)^2 (1 + \tau^2 x(s_0)^2))^{3/2}} z''(s_0).$$

Since  $\mathfrak{h}$  and  $x'(s_0) = y(s_0)$  are positive, we see that  $z''(s_0)$  is positive as well which yields that  $z(s_0)$  is a local minimum of  $z(s)$ . Thus,  $z(s)$  is increasing for  $s > s_0$  and decreasing for  $s < s_0$ . This behavior implies that the orbit describing  $\alpha(s)$  lies in  $\Theta_1$  for  $s > s_0$  and in  $\Theta_{-1}$  for  $s < s_0$ . Hence, this orbit in  $\Theta_{-1}$  ends at  $(x_0, y_0) \in \Omega^+$  and then starts at the same point but this time in  $\Theta_1$ .

If  $\gamma(s_0) \in \Omega^-$ , the proof is similar; just note that  $x'(s_0) = y_0 < 0$ , hence  $z''(s_0)$  is negative. This time, the orbit in  $\Theta_1$  ends at  $\Omega^-$  and then starts at the same point but this time in  $\Theta_{-1}$ .  $\square$

In any of these situations, i.e. where  $z'(s) = 0$  and it changes its monotony, we will say that the orbit in  $\Theta_\varepsilon$  *continues* in  $\Theta_{-\varepsilon}$ . and this continuation has to be understood as the extension of the associated  $\mathfrak{h}$ -surface having a common point with the same unit normal.

Finally, we focus on whether an orbit can *escape* from the phase plane  $\Theta_\varepsilon$ .

**Theorem 3.8** *Let be  $\mathfrak{h} \in \mathfrak{C}^1$  and  $\gamma(s) = (x(s), y(s))$  an orbit in  $\Theta_\varepsilon$ .*

- *If  $\kappa \leq 0$ , then  $x(s)$  cannot diverge to  $\infty$  if  $\kappa = 0$ , or tend to  $2/\sqrt{-\kappa}$  if  $\kappa < 0$ .*
- *If  $\kappa > 0$ , then  $x(s)$  cannot diverge to  $\infty$  in  $\Theta_1$ .*

*Proof:* The proof will be done by contradiction and distinguishing the possible values of  $\kappa$ .

**Case  $\kappa < 0$ .**

Let  $\alpha(s) = (x(s), 0, z(s))$  be the arc-length parametrized curve generated by  $\gamma(s)$ . Then, the fact that  $\alpha(s)$  is the profile of a rotational  $\mathfrak{h}$ -surface is equivalent to the following system to be fulfilled

$$\left\{ \begin{array}{l} x'(s) = \frac{\cos \theta(s)}{\sqrt{1 + \tau^2 x(s)^2}} \\ z'(s) = \frac{4 \sin \theta(s)}{4 + \kappa x(s)^2} \\ \theta'(s) = \frac{1}{(4 + \kappa x(s)^2) \sqrt{1 + \tau^2 x(s)^2}} \left( 8\mathfrak{h} \left( \frac{\cos \theta(s)}{\sqrt{1 + \tau^2 x(s)^2}} \right) - \frac{4 - \kappa x(s)^2}{x(s)} \sin \theta(s) \right), \end{array} \right. \quad (3.8)$$

Here,  $\theta(s)$  is the angle that  $\alpha'(s)$  makes with the  $E_1$ -direction.

Assume that  $\gamma(s)$  lies in  $\Theta_1$  with  $x(s) \rightarrow 2/\sqrt{-\kappa}$ ,  $s \nearrow s_0$ ; the case where  $s \searrow s_0$  or  $\gamma(s)$  lies in  $\Theta_{-1}$  are proved similarly. Hence,  $\gamma(s)$  is contained in  $\Lambda_1^+$  and stays there as  $x(s) \rightarrow 2/\sqrt{-\kappa}$  and  $y(s) \rightarrow y_0$ , where  $y_0 \in [0, 1/\sqrt{1 - 4\tau^2/\kappa}]$ . In particular,  $\theta(s) \rightarrow \theta_0 \in [0, \pi/2]$ , where  $\theta_0$  is defined by  $y_0 \sqrt{1 - 4\tau^2/\kappa} = \cos \theta_0$ . Because  $\mathfrak{h} \in \mathfrak{C}^1$ , at the limit  $x_0 := 2/\sqrt{-\kappa}$  we have

$$\frac{2}{\sqrt{-\kappa}} \mathfrak{h} \left( \frac{\cos \theta_0}{\sqrt{1 + \tau^2 x_0^2}} \right) > \sqrt{1 - \left( \frac{\cos \theta_0}{\sqrt{1 + \tau^2 x_0^2}} \right)^2} = \sqrt{\frac{\sin^2 \theta_0 + \tau^2 x_0^2}{1 + \tau^2 x_0^2}}.$$

Now, it is trivial to check that the following inequality holds

$$\mathfrak{h} \left( \frac{\cos \theta_0}{\sqrt{1 + \tau^2 x_0^2}} \right) - \frac{\sqrt{-\kappa}}{2} \sin \theta_0 \geq \mathfrak{h} \left( \frac{\cos \theta_0}{\sqrt{1 + \tau^2 x_0^2}} \right) - \frac{\sqrt{-\kappa}}{2} \sqrt{\frac{\sin^2 \theta_0 + \tau^2 x_0^2}{1 + \tau^2 x_0^2}} := c_0 > 0.$$

Taking limit we conclude

$$\lim_{s \rightarrow s_0} 8\mathfrak{h} \left( \frac{\cos \theta(x)}{\sqrt{1 + \tau^2 x^2}} \right) - \frac{4 - \kappa x^2}{x} \sin \theta(x) = 8 \left( \mathfrak{h} \left( \frac{\cos \theta_0}{\sqrt{1 + \tau^2 x_0^2}} \right) - \frac{\sqrt{-\kappa}}{2} \sin \theta_0 \right) \geq 8c_0 > 0,$$

So, the third equation in (3.8) yields that for  $x$  close to  $2/\sqrt{-\kappa}$  we have  $\theta'(s) \geq c_1/(4+\kappa x(s)^2)$ , for another positive constant  $c_1$ . In particular,  $\lim_{s \rightarrow s_0} \theta'(s) = \infty$ .

Now, we see the angle  $\theta$  as a function  $\theta(x)$  of  $x$ ; this can be done since  $x'(s) > 0$  and by the inverse function theorem. Hence,

$$\theta'(s) = \frac{d\theta}{ds} = \frac{d\theta}{dx} \frac{dx}{ds} = \theta'(x)x'(s) = \theta'(x) \frac{\cos \theta(x)}{\sqrt{1 + \tau^2 x^2}}.$$

In this setting, the third equation in (3.8) for  $x$  close enough to  $2/\sqrt{-\kappa}$  reads as:

$$\theta'(x) \cos \theta(x) = \frac{1}{4 + \kappa x^2} \left( 8\mathfrak{h} \left( \frac{\cos \theta(x)}{\sqrt{1 + \tau^2 x^2}} \right) - \frac{4 - \kappa x^2}{x} \sin \theta(x) \right) \geq \frac{c_1}{4 + \kappa x^2}.$$

Integrating from some fixed, large enough  $x_0$  and  $x$  yields

$$\sin \theta(x) \geq \frac{c_1}{2\sqrt{-\kappa}} \operatorname{arctanh} \left( \frac{\sqrt{-\kappa}}{2} x \right) + \sin \theta(x_0).$$

This is a contradiction since the right-hand side tends to infinity as  $x$  approaches to  $2/\sqrt{-\kappa}$ .

Following the idea developed for the case  $\kappa < 0$ , the cases  $\kappa \geq 0$  are proved similarly. Now, the  $x$ -coordinate of an orbit  $\gamma(s) = (x(s), y(s)) \in \Theta_\varepsilon$  would satisfy  $x(s) \rightarrow \infty$ . We give a sketch of the proof.

**Case  $\kappa = 0$ .** Suppose that  $\gamma(s)$  is in the phase plane  $\Theta_1$ ; the case  $\Theta_{-1}$  is analogous. Moreover, we assume that  $\gamma(s)$  is strictly contained in  $\Lambda_1^+$ , since the case when  $\gamma(s)$  lies in  $\Lambda_2^+$  is equivalent by symmetry of  $\Theta_1$ . After expressing  $\theta$  as a function of  $x$ , the third equation in (3.8) for  $x$  large enough yields

$$\theta'(x) \cos \theta(x) = 2\mathfrak{h} \left( \frac{\cos \theta(x)}{\sqrt{1 + \tau^2 x^2}} \right) - \frac{\sin \theta(x)}{x} \geq c_0 > 0.$$

Explicit integration from some  $x_0$  large enough and  $x > x_0$  yields  $\sin \theta(x) \geq c_0 x + \sin \theta(x_0)$ , which is obviously a contradiction when  $x \rightarrow \infty$ .

**Case  $\kappa > 0$ .** Finally, suppose that  $\gamma(s)$  belongs to  $\Theta_1$  and satisfies  $x(s) \rightarrow \infty$ . In this case,  $\theta(s) \rightarrow \theta_0 \in (0, \pi]$ . If we further assume that  $\gamma(s)$  lies in  $\Lambda_1^+$ , then  $\theta_0 \in (0, \pi/2]$ . Hence, the third equation in (3.8) for  $\kappa > 0$  yields

$$\theta'(x) \cos \theta(x) = \frac{1}{x} \left( \frac{x}{4 + \kappa x^2} \mathfrak{h} \left( \frac{\cos \theta(x)}{\sqrt{1 + \tau^2 x^2}} \right) + \frac{\kappa x^2 - 4}{\kappa x^2 + 4} \sin \theta(x) \right) \geq \frac{c_0}{x}, \quad c_0 > 0.$$

Again, integrating from  $x_0$  and  $x$  we conclude  $\sin \theta(x) \geq c_0 \log x + \sin \theta(x_0)$ , which is again a contradiction when  $x \rightarrow \infty$ .

Note that the fact that  $\gamma \in \Theta_1$  is fundamental to conclude that  $c_0 > 0$  (since  $\sin \theta_0 > 0$ ) and reach to the desired contradiction. Also, recall that when  $\tau > 0$ , i.e. in  $\mathbb{S}_b^3(\kappa, \tau)$ , the structure of  $\Theta_1$  implies that  $y(s) \rightarrow 0$  and hence  $\theta_0 = \pi/2$ .  $\square$

For  $\kappa \leq 0$  Theorem 3.8 yields that no entire, vertical  $\mathfrak{h}$ -graph exists, generalizing this well-known fact for CMC surfaces for the more general setting that  $\mathfrak{h} \in \mathfrak{C}^1$ . For  $\kappa > 0$  this implies that no  $\mathfrak{h}$ -surface generated by an orbit in  $\Theta_1$  converges to the antipodal fiber.

The only missing case is for  $\kappa > 0$  and  $\Theta_{-1}$ . In the next section we focus on the geometry of  $\mathbb{E}(\kappa, \tau)$  spaces having compact base, and deduce that some orbits tend to escape from  $\Theta_{-1}$ .

#### 4 Spaces with positive curvature

In this section we focus on the geometry of the  $\mathbb{E}(\kappa, \tau)$  spaces with  $\kappa > 0$ . Recall that the model  $\mathcal{R}(\kappa, \tau)$  misses to cover a fiber of the corresponding  $\mathbb{E}(\kappa, \tau)$  space. Thus, the main issue when studying the behavior of an orbit in the phase plane is that its  $x$ -coordinate may tend to infinity, hence the rotational  $\mathfrak{h}$ -surface would converge to the omitted *antipodal fiber*. We distinguish between the cases  $\tau = 0$  and  $\tau > 0$ .

**4.1. The space  $\mathbb{S}^2(\kappa) \times \mathbb{R}$ .** Let be  $p \in \mathbb{S}^2(\kappa) \times \mathbb{R}$  and suppose that the axis of rotation is the fiber  $\pi^{-1}(p_N) = \{p_N\} \times \mathbb{R}$ , where  $p_N$  is the north pole in  $\mathbb{S}^2(\kappa)$ . Denote by  $\beta_0$  to half of the the great circle in  $\mathbb{S}^2(\kappa)$  containing the points  $\{p_N, p_S\}$ , by  $\beta_1$  to the equator equidistant to  $p_N$  and  $p_S$ , and by  $q = \beta_0 \cap \beta_1$ . Define  $R_{\beta_1}$  to be the rotation in  $\mathbb{S}^2(\kappa) \times \mathbb{R}$  that sends the point  $p_N$  to  $p_S$  and fixes  $\beta_0$ . The image of a point  $X \in \mathbb{S}^2(\kappa) \times \mathbb{R}$  will be denoted by  $R_{\beta_1}(X) = \tilde{X}$ . The restriction of  $R_{\beta_1}$  to the set  $\beta_0 \times \mathbb{R}$  is just the reflection in  $\beta_0 \times \mathbb{R}$  with respect to the line  $\{q\} \times \mathbb{R}$ .

Next, consider the coordinate model  $\mathcal{R}(\kappa, \tau)$  introduced in Section 2.1. as

$$\Phi = \pi_{ster} \times \text{id}_{\mathbb{R}} : (\mathbb{S}^2(2/\sqrt{\kappa}) - \{p_S\}) \times \mathbb{R} \rightarrow \mathcal{R}(\kappa, \tau),$$

where  $\pi_{ster} : \mathbb{S}^2(2/\sqrt{\kappa}) - \{p_S\} \rightarrow \mathbb{R}^2$  is the stereographic projection and  $\text{id}_{\mathbb{R}}$  is the identity map. Moreover, we can assume without losing generality that  $\Phi(\beta_0 - \{p_S\})$  is the  $xz$ -plane in  $\mathcal{R}(\kappa, \tau)$ .

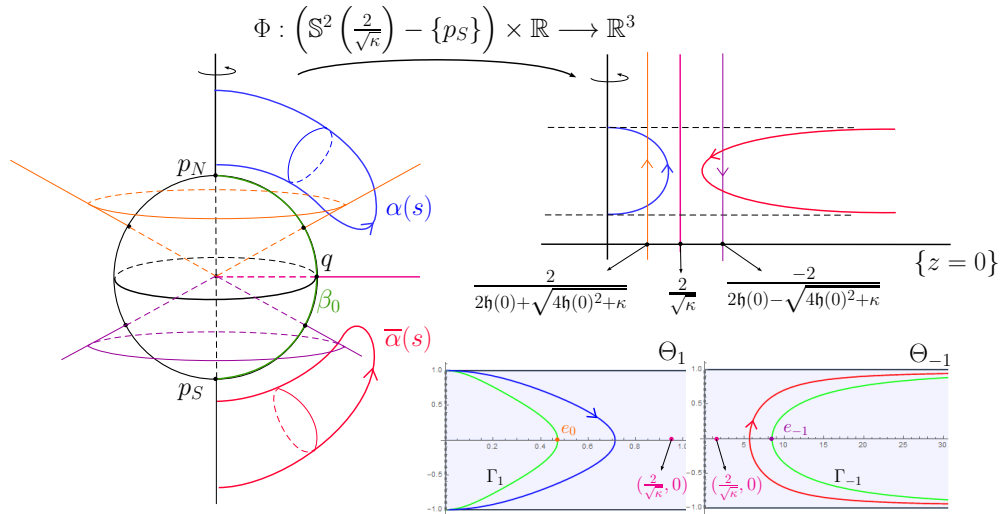


Figure 3: Left: a representation of the space  $\mathbb{S}^2(\kappa) \times \mathbb{R}$ . Right, top: stereographic projection of the profile curve. Right, bottom: the phase plane  $\Theta_\varepsilon$  and the associated orbits.

Let  $\alpha(s)$  be an arc-length parametrized curve in  $\beta_0 \times \mathbb{R}$  not intersecting the antipodal

axis  $\{p_S\} \times \mathbb{R}$  and  $\tilde{\alpha}(s)$  its image under  $R_{\beta_1}$ . We consider the projections  $\Phi(\alpha)$ ,  $\Phi(\tilde{\alpha})$  onto  $\{y = 0\}$ , and in order to save notation we will keep denoting them by  $\alpha, \tilde{\alpha}$ . If we compute the curvatures of  $\alpha$  and  $\tilde{\alpha}$  with respect to the unit normals  $J\alpha$  and  $J\tilde{\alpha}$ , we see that they are related as  $k_\alpha(s) = -k_{\tilde{\alpha}(s)}$ . So, if we consider the curve  $\bar{\alpha}(s) := \tilde{\alpha}(-s)$ , that is, we move backwards in  $s$ , we obtain  $k_{\bar{\alpha}(s)} = k_\alpha(s)$ ; see Figure 3, left.

This has the following implication when studying rotational  $\mathfrak{h}$ -surfaces in  $\mathbb{S}^2(\kappa) \times \mathbb{R}$ . If  $\alpha(s) = (x(s), 0, z(s)) \subset \beta_0 \times \mathbb{R}$  is an arc-length parametrized curve that generates an  $\mathfrak{h}$ -surface  $\Sigma_\alpha$ , the surfaces  $\Sigma_{\bar{\alpha}}$  and  $\Sigma_\alpha$  have the same mean curvature function and they differ by the isometry  $R_{\beta_1}$ . As a matter of fact, if  $\alpha(s)$  has increasing height function then it generates an orbit  $\gamma_1$  in  $\Theta_1$ , and so  $\bar{\alpha}(s)$  has decreasing height function and generates an orbit  $\gamma_{-1}$  in  $\Theta_{-1}$ . For example, this happens for the equilibrium points  $e_0 \in \Theta_1$  and  $e_{-1} \in \Theta_{-1}$ . They generate vertical lines that correspond to vertical cylinders in  $\mathbb{S}^2(\kappa) \times \mathbb{R}$  with the same constant mean curvature, one parametrized with increasing height (the one corresponding to  $e_0$ ) while the other has decreasing height (the one corresponding to  $e_{-1}$ ); see Figure 3, right.

Another example of this behavior is the following. For each  $H_0 > 0$  there exists a rotational sphere in  $\mathbb{S}^2(\kappa) \times \mathbb{R}$  with CMC equal to  $H_0$ . The corresponding arc-length parametrized curve  $\alpha(s)$  intersects the axis of rotation  $\{p_N\} \times \mathbb{R}$  orthogonally and has strictly increasing height function, i.e. it generates an orbit in the phase plane  $\Theta_1$ . Thus, the curve  $\bar{\alpha}(s)$  intersects orthogonally the antipodal axis  $\{p_S\} \times \mathbb{R}$ , has strictly decreasing height function and generates an orbit in the phase plane  $\Theta_{-1}$ . Both spheres agree under the isometry  $R_{\beta_1}$ . See Figure 3.

**4.2. The Berger spheres.** Consider the 3-dimensional sphere  $\mathbb{S}^3 := \{(v, w) \in \mathbb{C}^2; |v|^2 + |w|^2 = 1\}$  and the vector field  $\hat{\xi} = (iv, iw)$ . Then, the Berger sphere  $\mathbb{S}_b^3(\kappa, \tau)$  is  $\mathbb{S}^3$  endowed with the metric

$$g(X, Y) = \frac{4}{\kappa} \left( \langle X, Y \rangle + \left( \frac{4\tau^2}{\kappa} - 1 \right) \langle X, \hat{\xi} \rangle \langle Y, \hat{\xi} \rangle \right),$$

where  $\langle \cdot, \cdot \rangle$  is the usual flat metric in  $\mathbb{C}^2$ . In particular, when  $\kappa = 4\tau^2$  we recover the usual 3-sphere with a homothetic metric.

We denote by  $\mathbb{S}^2(\kappa)$  to the 2-sphere of constant curvature  $\kappa > 0$ , viewed as the set of points  $p \in \mathbb{R}^3$  such that  $|p|^2 = 1/\kappa$ . Then, the Hopf fibration  $\Pi : \mathbb{S}_b^3(\kappa, \tau) \rightarrow \mathbb{S}^2(\kappa)$

$$\Pi(v, w) = \frac{2}{\sqrt{\kappa}} \left( v\bar{w}, \frac{1}{2}(|v|^2 - |w|^2) \right),$$

is a Riemannian submersion whose kernel is precisely the vector field  $\hat{\xi}$  of constant length. Hence,  $\Pi$  is isomorphic to the canonical projection of  $\mathbb{E}(\kappa, \tau)$ , and  $\xi = \hat{\xi}/|\hat{\xi}|$  is the associated Killing vector field.

Now we describe the coordinates  $(x, y, z)$  of the local model  $\mathcal{R}(\kappa, \tau)$  introduced at the beginning of Section 2. The first two coordinates correspond to the inverse stereographic projection

$$\zeta(x, y) = \left( \lambda x, \lambda y, \frac{1}{\sqrt{\kappa}}(1 - 2\lambda) \right) : \mathbb{R}^2 \rightarrow \mathbb{S}^2(\kappa) - \{(0, 0, 1/\sqrt{\kappa})\}, \quad \lambda = \frac{1}{1 + \frac{\kappa}{4}(x^2 + y^2)}.$$

The third coordinate  $z$  of each point  $(x, y, z) \in \mathcal{R}(\kappa, \tau)$  is the unit speed of the fiber  $\Pi^{-1}(\zeta(x, y))$ . If we assume the axis of rotation in  $\mathcal{R}(\kappa, \tau)$  to be the line  $(0, 0, z)$ , then the fiber of rotation in  $\mathbb{S}_b^3(\kappa, \tau)$  is  $\Pi^{-1}(\zeta(0, 0)) = \Pi^{-1}((0, 0, -1/\sqrt{\kappa}))$ , that is the fiber  $F := (0, e^{i\theta})$ ,  $\theta \in \mathbb{R}$ . For instance, the fiber in  $\mathbb{S}_b^3(\kappa, \tau)$  that the model  $\mathcal{R}(\kappa, \tau)$  omits is just  $\Pi^{-1}((0, 0, 1/\sqrt{\kappa}))$ , i.e. the fiber  $F^* := (e^{i\theta}, 0)$ ,  $\theta \in \mathbb{R}$ . An explicit isometry between  $\mathcal{R}(\kappa, \tau)$  and  $\mathbb{S}_b^3(\kappa, \tau) - \{(e^{i\theta}, 0)\}$  is given by

$$\Psi : (x, y, z) \mapsto \frac{1}{\sqrt{1 + \frac{\kappa}{4}(x^2 + y^2)}} \left( \frac{\sqrt{\kappa}}{2}(x + iy)e^{i\frac{\kappa}{4\tau}z}, e^{i\frac{\kappa}{4\tau}z} \right). \quad (4.1)$$

With this isometry we see that two points  $(x, y, z)$  and  $(x, y, z + 8\tau\pi/\kappa)$  are identified to the same point in  $\mathbb{S}_b^3(\kappa, \tau)$ . A local inverse of  $\Psi$  between  $\mathbb{S}_b^3(\kappa, \tau) - \{(e^{i\theta}, 0)\}$  and  $\mathcal{R}(\kappa, \tau)$  is

$$\Psi^{-1}(v, w) = \left( \frac{2}{\sqrt{\kappa}} \frac{1}{|w|^2} \operatorname{Re}(v\bar{w}), \frac{2}{\sqrt{\kappa}} \frac{1}{|w|^2} \operatorname{Im}(v\bar{w}), \frac{4\tau}{\kappa} \operatorname{arg}(w) \right).$$

Recall that if  $\Sigma$  is a surface in  $\mathbb{S}_b^3(\kappa, \tau)$  invariant by the group of rotations  $Rot$  around the fiber  $F = (0, e^{i\theta})$ , then  $\mathbb{S}_b^3(\kappa, \tau)/Rot$  is diffeomorphic to  $\mathbb{S}^2$ , and so  $\Sigma$  is just the image of a curve  $\alpha$  in  $\mathbb{S}^2$  under  $Rot$ . By rotational symmetry it suffices to just consider  $\alpha$  in the half-sphere  $\overline{\mathbb{S}_+^2}$ , where  $\partial\mathbb{S}_+^2 = F$ . For example, if  $(w, a) \subset \mathbb{C} \times \mathbb{R}$  are the coordinates of a 2-sphere in  $\mathbb{R}^3$ , then the immersion

$$G(w, a) = (a, 0, w) : \mathbb{S}^2 \rightarrow \mathbb{S}_b^3(\kappa, \tau)$$

is a minimal sphere whose equator  $G(w, 0)$  agrees with the fiber of rotation  $F$ . Hence, rotational surfaces in  $\mathbb{S}_b^3(\kappa, \tau)$  are in correspondence with curves in the half-sphere  $G(w, a)$ ,  $a \geq 0$ . As a matter of fact, the profile curve of a rotational surface around  $F$  can be parametrized by  $\alpha(s) = (\sin x(s), 0, \cos x(s)e^{iz(s)})$ .

Notice that the image of the set  $G(\cos \theta, 0, \sin \theta)$  under  $\Psi^{-1}$  is the line  $(x, 0, 0)$ ,  $x > 0$  for  $\theta \in [0, \pi/2)$ , and the line  $(x, 0, 4\pi\tau/\kappa)$ ,  $x < 0$  for  $\theta \in (\pi/2, \pi]$ . Finally, note that  $G(0, 0, 1) = (1, 0, 0) \in F^*$  is the limit point  $\lim_{x \rightarrow \infty} \Psi(x, 0, 0)$ , and in general

$$\lim_{r \rightarrow \infty} \Psi(r \cos \theta_0, r \sin \theta_0, 0) = \lim_{r \rightarrow \infty} \frac{1}{\sqrt{1 + \frac{\kappa}{4}r^2}} \left( \frac{\sqrt{\kappa}}{2} r e^{i\theta_0}, 1, 0 \right) = (e^{i\theta_0}, 0).$$

From now on, the point  $p_N := (1, 0, 0)$  will be the *north pole* of  $\mathbb{S}_b^3(\kappa, \tau)$ .

The subset  $\mathfrak{Z}$  in  $\mathcal{R}(\kappa, \tau)$  such that  $\Psi(\mathfrak{Z})$  lies in  $G(\mathbb{S}^2)$  is the set of points  $(x, y, z) \in \mathcal{R}(\kappa, \tau)$  such that  $\Psi(x, y, z) \subset G(\mathbb{S}^2) = \{(a, 0, w); a \in \mathbb{R}, w \in \mathbb{C}, a^2 + |w|^2 = 1\}$  satisfy

$$x \sin \frac{\kappa z}{4\tau} + y \cos \frac{\kappa z}{4\tau} = 0.$$

Thus, the orbit space in  $\mathcal{R}(\kappa, \tau)$  that is identified with the orbit space  $\overline{\mathcal{S}_+} \subset \mathbb{S}_b^3(\kappa, \tau)$  is a minimal helicoid. Since the helicoid and the  $xz$ -plane are 1-1 under the group of rotations leaving pointwise fixed the  $E_3$ -axis, such a plane will be considered to be the orbit space of rotational surfaces in  $\mathcal{R}(\kappa, \tau)$ .

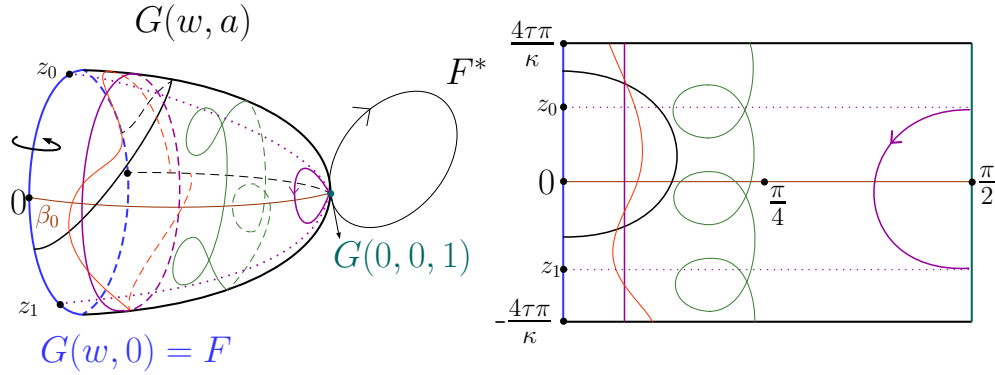


Figure 4: The profile curves of rotational CMC surfaces in Berger spheres  $\mathbb{S}_b^3(\kappa, \tau)$ .

As a matter of fact, the structure of the rotational surfaces with positive, constant mean curvature in  $\mathbb{S}_b^3(\kappa, \tau)$  is represented in Figure 4. See [Tor] for a detailed description of these surfaces. In particular, the orbit corresponding to the profile curve starting from the north pole  $p_N$  appears in the phase plane  $\Theta_{-1}$  of Equation (3.4) when  $\mathfrak{h}$  is a positive constant  $H_0$ .

## 5 Proof of Theorem 1.3

**5.1. A Delaunay-type classification.** This section is devoted to prove Theorem 1.3.

*Proof:* We will use the coordinate model  $\mathcal{R}(\kappa, \tau)$  as introduced in Section 2, which is a global model when  $\kappa \leq 0$ . When  $\kappa > 0$ ,  $\mathcal{R}(\kappa, \tau)$  omits the fiber  $\{p_S\} \times \mathbb{R}$  in  $\mathbb{S}^2(\kappa) \times \mathbb{R}$ , and the fiber  $F^* = (e^{i\theta}, 0)$  in  $\mathbb{S}_b^3(\kappa, \tau)$ ; see Section 4 for details. We suppose that the axis of rotation is the  $E_3$ -axis  $(0, 0, z)$ ,  $z \in \mathbb{R}$ .

The proof will be done by taking advantage from the phase plane analysis made in Section 3. The structure of the phase planes  $\Theta_\varepsilon$ ,  $\varepsilon = \pm 1$ , for the different cases  $\kappa, \tau$  was shown in Figure 2 and detailed in Proposition 3.2. In particular, the equilibrium point  $e_0$  in  $\Theta_1$  given by Equation (3.5) generates a CMC vertical cylinder, obtaining the first example of the classification. Note that the equilibrium  $e_{-1}$  given by Equation (3.6) exists in  $\Theta_{-1}$  for  $\kappa > 0$ ; it generates a CMC cylinder with the same constant mean curvature  $\mathfrak{h}(0)$  that agrees with the one generated by  $e_0$  after an ambient isometry.

For the existence of the  $\mathfrak{h}$ -sphere, consider the orbit  $\gamma_+$  starting at the point  $(0, 1)$  at the instant  $s = 0$  given by Proposition 3.6. For  $s > 0$  small enough  $\gamma_+(s)$  lies in  $\Lambda_1^+$ , and from Propositions 3.7 and 3.8 we conclude that  $\gamma_+(s)$  is contained in  $\Lambda_1^+$  until it intersects the axis  $y = 0$  at some  $\gamma(s_0) = (r_0, 0)$ ,  $r_0 > 0$ . This also holds for the orbit  $\gamma_-(s)$ , i.e. this time  $\gamma_-(s)$  ends at the point  $(0, -1)$  at some instant  $s_1 > 0$ , is contained in  $\Lambda_2^+$  and comes from intersecting the axis  $y = 0$  at a finite instant. Since  $\gamma_+$  and  $\gamma_-$  are symmetric, they meet orthogonally at the axis  $y = 0$ . By uniqueness  $\gamma_+$  and  $\gamma_-$  can be smoothly glued to generate a compact orbit  $\gamma_0 := \gamma_+ \cup \gamma_-$  that joins the points  $(0, 1)$  and  $(0, -1)$ .

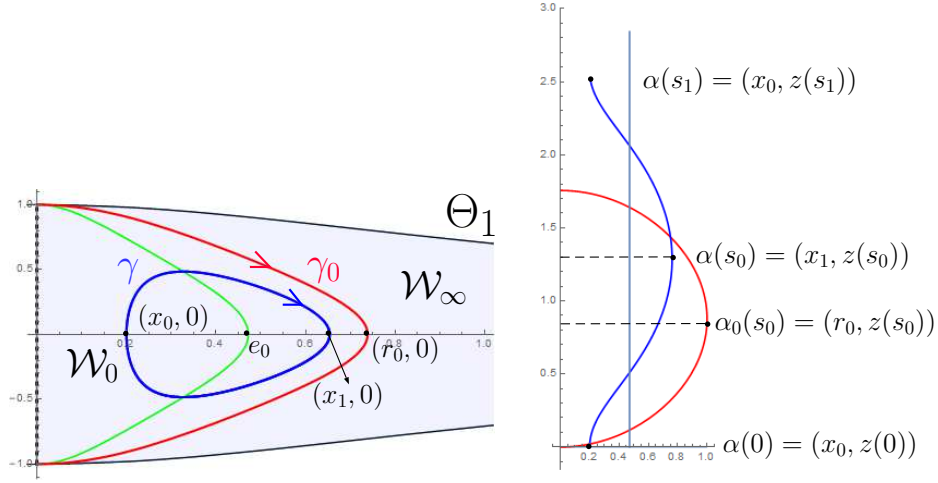


Figure 5: Left: the phase plane  $\Theta_1$  and the orbits corresponding to the  $\mathfrak{h}$ -sphere, the CMC cylinder and an  $\mathfrak{h}$ -unduloid. Right, the profile curves of these  $\mathfrak{h}$ -surfaces.

The arc-length parametrized curve  $\alpha_0(s)$  associated to  $\gamma_0(s)$  intersects the  $E_3$ -axis at the instant  $s = 0$ , has strictly increasing height function (hence is embedded in  $\mathcal{R}(\kappa, \tau)$ ), and its angle function at the instant  $s = s_0$  vanishes; here, the  $x(s)$ -coordinate reaches a global maximum and then decreases. By the even condition on  $\mathfrak{h}$ ,  $\alpha_0$  is symmetric with respect to the horizontal geodesic at height  $z(s_0)$  in the  $xz$ -plane. The  $\mathfrak{h}$ -surface generated by rotating  $\alpha_0$  is an  $\mathfrak{h}$ -sphere, denoted by  $S_{\mathfrak{h}}$ , with strictly decreasing angle function. See Figure 5.

Recall that the orbit  $\gamma_0$  of the  $\mathfrak{h}$ -sphere divides  $\Theta_1$  in two connected components: one bounded containing the equilibrium  $e_0$ , that we will denote by  $\mathcal{W}_0$ , and other unbounded that we will denote by  $\mathcal{W}_\infty$ .

To prove the existence of the  $\mathfrak{h}$ -unduloids, consider  $x_0 > 0$  such that  $(x_0, 0) \in \mathcal{W}_0$ , and suppose that  $(x_0, 0)$  is at the left-hand side of  $e_0$ . Let  $\gamma(s) = (x(s), y(s))$  be the orbit passing through  $(x_0, 0)$  at the instant  $s = 0$ . Then, for  $s > 0$  small enough  $\gamma(s)$  is contained in  $\Lambda_4^+$  and follows its monotonicity direction. By continuity,  $\gamma(s)$  has to intersect  $\Gamma_1$  at some finite point, where the  $y(s)$ -coordinate of  $\gamma(s)$  reaches a maximum, and then  $\gamma(s)$  enters to the region  $\Lambda_1^+$ . Since  $\gamma(s)$  cannot intersect  $\gamma_0$  by uniqueness of the Cauchy problem and  $\gamma(s)$  cannot converge to  $e_0$  with  $s \rightarrow \infty$  in virtue of Proposition 3.3, the only possibility for  $\gamma(s)$  is to intersect the axis  $y = 0$  at some finite point  $\gamma(s_0) = (x_1, 0)$  lying at the right-hand side of  $e_0$ . By symmetry of  $\Theta_1$ , the same behavior holds in the regions  $\Lambda_2^+$  and  $\Lambda_3^+$  and then  $\gamma(s)$  reaches again the point  $(x_0, 0)$  at some instant  $s_1 > 0$ , which implies that  $\gamma(s)$  is a periodic orbit. Note that in any case,  $\gamma(s)$  cannot converge to the segment  $\{0\} \times [-1, 1]$  in virtue of Proposition 3.4.

This orbit generates an arc-length parametrized curve  $\alpha(s)$  whose height function is strictly increasing (since  $\gamma(s) \subset \Theta_1$ ) and hence  $\alpha(s)$  is embedded. The  $x(s)$ -coordinate of  $\alpha(s)$  is periodic, its maximum is  $x(s_0) = x_1$  and its minimum is  $x(0) = x_0$ ; see Figure 5. The rotation of  $\alpha(s)$  generates a properly embedded  $\mathfrak{h}$ -surface  $U_{\mathfrak{h}}$  that is diffeomorphic to  $\mathbb{S}^1 \times \mathbb{R}$  and with periodic distance to the  $E_3$ -axis, that is,  $U_{\mathfrak{h}}$  is an  $\mathfrak{h}$ -unduloid.



Moreover, each  $\mathfrak{h}$ -unduloid is uniquely determined by the value  $x_0$  that agrees with the radius of the smallest circumference contained in  $U_{\mathfrak{h}}$ . Thus, the family of  $\mathfrak{h}$ -unduloids is a continuous family  $\{U_{\mathfrak{h}}(r)\}$  parametrized by the *necksize* of their *waists*, where  $0 < r < 2(\sqrt{4\mathfrak{h}(0)^2 + \kappa} + 2\mathfrak{h}(0))^{-1}$ . Similarly to the CMC case, when  $r \rightarrow 2(\sqrt{4\mathfrak{h}(0)^2 + \kappa} + 2\mathfrak{h}(0))^{-1}$  the  $\mathfrak{h}$ -unduloids  $U_{\mathfrak{h}}(r)$  converge to the vertical cylinder of CMC  $\mathfrak{h}(0)$ , and when  $r \rightarrow 0$  the  $\mathfrak{h}$ -unduloids converge to a singular chain of tangent  $\mathfrak{h}$ -spheres.

Lastly, we prove the existence of the  $\mathfrak{h}$ -nodoids. For that, let  $(r_0, 0)$  be the point of intersection of  $\gamma_0$  with  $y = 0$ , and fix some  $x_0 > r_0$ . Consider the orbit  $\gamma(s)$  passing through  $(x_0, 0)$  at the instant  $s = 0$ . For  $s > 0$  small enough,  $\gamma(s)$  lies in  $\Lambda_2^+$ , and since  $\gamma_0$  and  $\gamma$  cannot intersect each other,  $\gamma(s)$  has some  $\gamma(s_0) = (x_1, y_1) \in \Omega^-$ ,  $x_1 > 0$ ,  $y_1 < 0$  as endpoint. By symmetry,  $\gamma(s)$  for  $s < 0$  has the same behavior at  $\Lambda_1^+$ , having the point  $\gamma(-s_0) = (x_1, -y_1) \in \Omega^+$  as endpoint. This orbit generates an arc-length parametrized curve  $\alpha(s)$  which is also symmetric with respect to the rotation of angle  $\pi$  around the horizontal geodesic in the  $xz$ -plane at height  $z(0)$ ; after a vertical translation we can suppose that  $z(0) = 0$ . At this height, the  $x(s)$ -coordinate of  $\alpha(s)$  reaches its maximum  $x_0$ , and then decreases to the value  $x_1$ . The height  $z(s)$  reaches a minimum at  $s = -s_0$  where  $z'(-s_0) = 0$ , then increases and reaches a maximum at  $s = s_0$  where again  $z'(s_0) = 0$ .

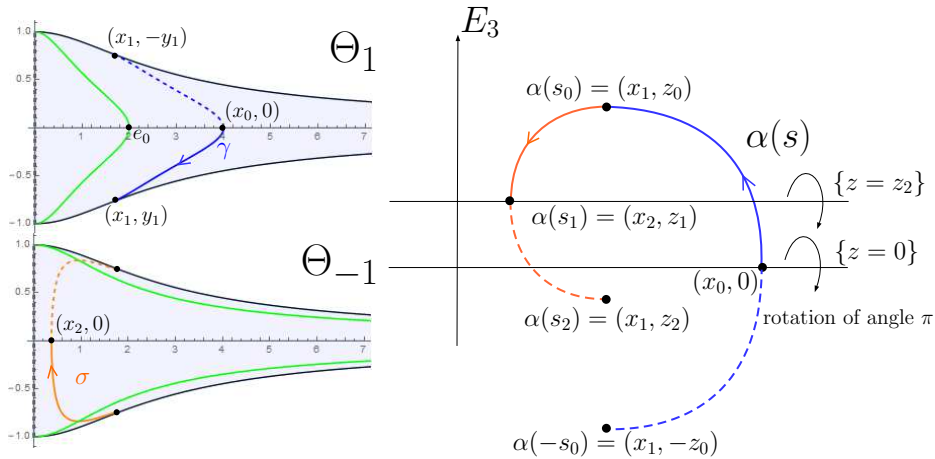


Figure 6: Left: the phase plane and the orbit generating an  $\mathfrak{h}$ -nodoid. Right: the profile curve of the  $\mathfrak{h}$ -nodoid.

Now, for  $s > s_0$  the function  $z(s)$  is decreasing, hence  $\alpha(s)$  for  $s > s_0$  generates an orbit  $\sigma(s)$  in  $\Theta_{-1}$  having the point  $(x_1, y_1) \in \Omega^-$  as endpoint. The monotonicity properties of  $\Theta_{-1}$  and Proposition 3.4 ensures us that  $\sigma(s)$  has to intersect the axis  $y = 0$  at some finite point  $\sigma(s_1) = (x_2, 0)$ ,  $x_2 > 0$ . By symmetry,  $\sigma(s)$  ends up having the point  $(x_1, -y_1) \in \Omega^+$  as endpoint for some  $s = s_2$ . Thus, the height of  $\alpha(s)$  is strictly decreasing starting at the value  $z_0$  and having the value  $z(s_2)$  as minimum. This time, the distance  $x(s)$  to the  $E_3$ -axis has the value  $x_2$  as minimum. See Figure 6.

Note that if  $z_2 = -z_0$ , the curve  $\alpha(s)$  is closed and generates a rotational  $\mathfrak{h}$ -torus. Note that no rotational  $\mathfrak{h}$ -tori can exist in  $\mathbb{H}^2(\kappa) \times \mathbb{R}$ , i.e. for  $\tau = 0$  and  $\kappa < 0$ , as a consequence of Alexandrov reflection technique with respect to vertical planes. In Section 6, which has

interest on itself, we discuss the existence of  $\mathfrak{h}$ -tori in  $\mathbb{E}(\kappa, \tau)$  spaces with  $\kappa \leq 0$  and  $\tau > 0$ .

For  $\tau = 0$  and  $\kappa > 0$ , we prove next the existence of an  $\mathfrak{h}$ -torus in  $\mathbb{S}^2(\kappa) \times \mathbb{R}$ . Consider an arc-length parametrized curve  $\alpha_T(s) = (x(s), 0, z(s))$  in  $\beta_0 \times \mathbb{R}$  such that  $\alpha_T(0) = (q, 0)$  and  $\alpha'_T(0)$  is orthogonal to  $\{q\} \times \mathbb{R}$  with angle function equal to 1. This curve generates an orbit  $\gamma_T(s)$  in  $\Theta_1$ , symmetric with respect to the axis  $y = 0$ , with starting point at  $\gamma_T(0) = (2/\sqrt{\kappa}, 1)$ , that intersects the axis  $y = 0$  at some  $\gamma_T(s_0) = (x_1, 0)$ ,  $x_1 > 2/\sqrt{\kappa}$ , and with endpoint  $\gamma_T(s_1) = (2/\sqrt{\kappa}, -1)$ . By symmetry of  $\gamma_T$ , the curve  $\alpha_T(s)$  is also symmetric with respect to  $\beta_0 \times \{z_0\}$ , where  $z_0 = z(s_0)$ . When  $\alpha_T(s)$  intersects orthogonally the fiber  $\{q\} \times \mathbb{R}$  at the point  $(q, z_1)$ ,  $z_1 = z(s_1)$ , it does with angle function equal to -1, then  $z(s)$  for  $s > s_1$  decreases and so  $\gamma_T(s)$  enters to the phase plane  $\Theta_{-1}$ .

Because  $\alpha_T(s)$  is symmetric with respect to  $\{q\} \times \mathbb{R}$ , it ends up at the point  $(q, 0)$  having angle function equal to 1. This ensures us that the orbit  $\gamma_T(s)$  in  $\Theta_{-1}$  is a compact arc, symmetric with respect to the axis  $y = 0$ , having the point  $(2/\sqrt{\kappa}, -1)$  as starting point and  $(2/\sqrt{\kappa}, 1)$  as endpoint. This configuration gives us an embedded, rotational  $\mathfrak{h}$ -torus.

Finally, we analyze the case when in a Berger sphere a solution approaches to the fiber  $F^* = (e^{i\theta}, 0)$  omitted by the model  $\mathcal{R}(\kappa, \tau)$ . Recall that the orbit  $\gamma_0$  of the  $\mathfrak{h}$ -sphere intersects the axis  $y = 0$  at  $(r_0, 0)$ . Consider an orbit  $\gamma$  in  $\Theta_1$  such that  $\gamma(0) = (r_1, 0)$  with  $r_1 > r_0$ . This orbit corresponds to an  $\mathfrak{h}$ -nodoid, hence is compact and enters to the phase plane  $\Theta_{-1}$  generating another compact orbit that intersects the axis  $y = 0$  at some  $(r_2, 0)$ . Moreover, as  $r_1$  increases  $r_2$  also increases. Thus, when  $r_1 \rightarrow \infty$  we conclude that  $r_2 \rightarrow r_\infty$  with  $r_\infty \leq 2 \left( \sqrt{4\mathfrak{h}(0)^2 + \kappa} - 2\mathfrak{h}(0) \right)^{-1}$ , that is  $(r_\infty, 0)$  lies at the left-hand side of  $e_{-1}$  or agrees with it.

Now, take some  $x_0 > 0$  and an orbit  $\gamma \subset \Theta_{-1}$  such that  $\gamma(0) = (x_0, 0)$  lies at the right-hand side of  $e_{-1}$ . Then,  $\gamma$  is a closed orbit that has  $e_{-1}$  in its inner region, and thus generates an  $\mathfrak{h}$ -unduloid that agrees after an ambient isometry with an  $\mathfrak{h}$ -unduloid generated by an orbit in  $\Theta_1$ . The orbit  $\gamma$  defines a unique point  $(x_1, 0)$ ,  $x_1 > 0$  at the left-hand side of  $e_{-1}$  where  $\gamma$  intersects the  $y = 0$  axis. In particular,  $x_1 > r_\infty$  and so  $(r_\infty, 0) \neq e_{-1}$ . Finally, recall that when  $x_0$  increases then  $x_1$  decreases and so  $x_1 \rightarrow x_\infty \geq r_\infty$  when  $x_0 \rightarrow \infty$ .

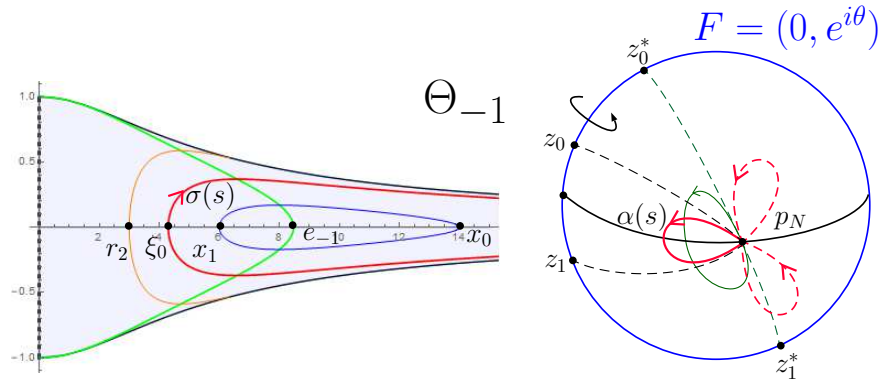


Figure 7: Left: the phase plane  $\Theta_{-1}$  for the Berger spheres. Right: the configuration of the profile curve that passes through the north pole  $p_N \in \mathbb{S}_b^3(\kappa, \tau)$  omitted in the model  $\mathcal{R}(\kappa, \tau)$ .

By continuity of the phase plane, any orbit  $\sigma(s) = (x(s), y(s))$  in  $\Theta_{-1}$  passing through some  $(\xi, 0)$  with  $\xi \in [r_\infty, x_\infty]$  is symmetric with respect to the axis  $y = 0$  and satisfies  $x(s) \rightarrow \infty$  and  $y(s) \rightarrow 0$  as  $s \rightarrow \pm\infty$ . This orbit generates a curve  $\alpha(s)$  that starts from the north pole  $p_N$  of  $\mathbb{S}_b^3(\kappa, \tau)$  at some instant  $s = s_0 < 0$  with vanishing angle function, and ends again at  $p_N$  at  $s = s_1 > 0$ . Since  $\alpha(s)$  is unique with this initial data, so it is  $\sigma$  in  $\Theta_{-1}$ , i.e.  $r_\infty = x_\infty := \xi_0$ . See Figure 7.

Let  $\Sigma$  be the  $\mathfrak{h}$ -surface generated by rotating  $\alpha(s)$  around the fiber  $F$ . The fact that  $\Sigma$  is compact or embedded depends on whether the curve  $\alpha(s)$  closes or not. For instance:

- If  $z_0 - z_1 = 4\pi\tau/\kappa$ , then  $\alpha'(s_0) = \alpha'(s_1)$  and so  $\alpha(s)$  closes when reaching the north pole at the instant  $s = s_1$ . Hence,  $\Sigma$  is an embedded  $\mathfrak{h}$ -torus.
- If  $z_0 - z_1$  is a rational multiple of  $4\pi\tau/\kappa$ , then  $\alpha'(s_0) \neq \alpha'(s_1)$  and so  $\alpha(s)$  has a cusp at  $p_N$ . The different branches of  $\alpha(s)$  are obtained by rotating  $\alpha(s)$  an angle  $z_1 - z_0$  around  $p_N$ . After a finite number of iterations,  $\alpha(s)$  closes with  $C^1$  regularity. Hence,  $\Sigma$  is an immersed  $\mathfrak{h}$ -torus with self-intersections.
- If  $z_0 - z_1$  is an irrational multiple of  $4\pi\tau/\kappa$ , then  $\alpha(s)$  never closes. Hence,  $\Sigma$  is an immersed, non-compact surface that is dense inside a solid torus.

Furthermore, suppose that the profile curve  $\alpha(s) = (\sin x(s), 0, \cos x(s)e^{iz(s)})$  closes at  $p_N$  with  $\alpha'(s_0) = \alpha'(s_1)$ . By restricting ourselves locally around  $p_N$  to  $\alpha(s)|_{[s_0-\varepsilon, s_0+\varepsilon]}$  for  $\varepsilon > 0$  small enough, we can express locally  $x$  as a function  $x(z)$ . Define  $\alpha_- := \alpha(s)|_{[s_0-\varepsilon]}$ ,  $\alpha_+ := \alpha(s)|_{[s_0+\varepsilon]}$ , and let  $\Sigma_+$  and  $\Sigma_-$  be the  $\mathfrak{h}$ -surfaces generated by  $\alpha_+$  and  $\alpha_-$  respectively. Then,  $\Sigma_\pm$  have at common boundary the great circle obtained by rotating  $p_N$  around  $F$ , where their unit normals agree. By the uniqueness of the Cauchy problem for rotational  $\mathfrak{h}$ -graphs,  $\Sigma_+$  and  $\Sigma_-$  can be smoothly glued along this boundary component. This proves that  $\alpha$  closes with  $C^2$  regularity at  $p_N$ , and so it does the union  $\Sigma_+ \cup \Sigma_-$  along their common boundary.  $\square$

**5.2. Embeddedness and compactness of  $\mathfrak{h}$ -surfaces in  $\mathbb{S}_b^3(\kappa, \tau)$ .** As pointed out in [Tor], CMC spheres in  $\mathbb{S}_b^3(\kappa, \tau)$  might be either embedded or immersed and have self-intersections. As a matter of fact, if the difference of the heights between the top and bottom points is greater than  $8\tau\pi/\kappa$ , then the sphere has self-intersections. This is a consequence from the fact that in the model  $\mathcal{R}(\kappa, \tau)$ , two points  $(x, y, z)$  and  $(x, y, z + 8\tau\pi/\kappa)$  are identified to the same point in  $\mathbb{S}_b^3(\kappa, \tau)$ , see Equation (4.1).

The same happens for  $\mathfrak{h}$ -surfaces. If the height between the top and bottom points of an  $\mathfrak{h}$ -sphere is less than  $8\tau\pi/\kappa$ , then the  $\mathfrak{h}$ -sphere is embedded. Otherwise, it has self-intersections. Unlike CMC surfaces, no first integral is known for  $\mathfrak{h}$ -surfaces and so an explicit expression of the height of its solutions.

This discussion also holds regarding the compactness of  $\mathfrak{h}$ -unduloids and  $\mathfrak{h}$ -nodoids. If the difference of heights  $T$  between consecutive periodic points is a rational multiple of  $8\tau\pi/\kappa$ , these solutions close and hence generate compact  $\mathfrak{h}$ -tori. Moreover, they are embedded if and only if  $T = \frac{8\tau\pi}{p\kappa}$ ,  $p \in \mathbb{Z}$ .

Finally, if  $T$  is an irrational multiple of  $8\tau\pi/\kappa$  then the corresponding  $\mathfrak{h}$ -unduloid or  $\mathfrak{h}$ -nodoid never closes, hence is not compact and is dense inside a solid torus.

## 6 Proof of Theorem 1.4

In this section we prove Theorem 1.4, where we discuss the existence and non-existence of rotational  $\mathfrak{h}$ -tori in the spaces  $\text{Nil}_3$  and  $\widetilde{SL}_2(\mathbb{R})$ .

**6.1. Non-existence of rotational  $\mathfrak{h}$ -tori.** We show the non-existence of rotational  $\mathfrak{h}$ -tori for further prescribed functions  $\mathfrak{h} \in \mathcal{C}^1$  that generalize the case that  $\mathfrak{h}$  is constant.

Suppose that  $\alpha(s) = (x(s), 0, z(s))$  in  $\mathcal{R}(\kappa, \tau)$  is arc-length parametrized with respect to the metric (3.2) and that generates an  $\mathfrak{h}$ -surface after being rotated around the  $E_3$ -axis. Then, as pointed out in Proposition 3.8, its coordinates satisfy Equation (3.8).

Now, suppose that  $\alpha(s)$  generates a compact portion of an  $\mathfrak{h}$ -nodoid as in showed in Figure 6. Hence,  $\alpha(s)$  is defined for  $s \in (0, s_1)$ , and satisfies  $\theta(0) = \pi/2$ ,  $\theta(s_0) = \pi$  and  $\theta(s_1) = 3\pi/2$ . In particular,  $\theta'(s) > 0$  for every  $s \in (0, s_1)$ . After a vertical translation, suppose that  $z(0) = 0$ .

From system (3.8), we have that the function  $z(s)$  can be written by the integral formula  $z(s) = \int_0^s 4 \sin \theta(t)/(4 + \kappa x(t)^2) dt$ . Because  $\theta'(s) > 0$ , we can express the functions  $x(s)$ ,  $z(s)$  and  $\nu(s)$  as functions of the angle  $\theta$ . The chain rule yields

$$\frac{dz}{d\theta} = \frac{z'(s)}{\theta'(s)} = \frac{4 \sin \theta \sqrt{1 + \tau^2 x^2}}{8\mathfrak{h}(\nu) - \frac{4 - \kappa x^2}{x} \sin \theta}.$$

Recall that the denominator has the same sign of  $\theta'(s)$ , hence it is positive everywhere. Thus, we have

$$I_1 := - \int_{\pi}^{3\pi/2} \frac{dz}{d\theta} d\theta = z(s_0) - z(s_1); \quad I_2 := \int_{\pi/2}^{\pi} \frac{dz}{d\theta} d\theta = z(s_0) - z(0). \quad (6.1)$$

and so  $z(s_1) > z(0)$  if and only if  $I_1 < I_2$ .

Choose  $s \in (0, s_0)$  and  $\bar{s} \in (s_0, s_1)$  such that  $\sin \theta(s) = -\sin \theta(\bar{s})$ ; in particular,  $x(s) > x(\bar{s})$ . Since  $\kappa \leq 0$ , the map  $x \mapsto f(x) := (4 - \kappa x^2)/x$  is positive and strictly decreasing for  $x < 2/\sqrt{-\kappa}$ ; when  $\kappa = 0$  this is fulfilled for every  $x > 0$ . As a matter of fact,  $f(x(s)) < f(x(\bar{s}))$ . Finally, since  $\nu(s) = \cos \theta(s)/\sqrt{1 + \tau^2 x(s)^2}$ , after a straightforward computation we conclude that  $\nu(s) > \nu(\bar{s})$ .

Now, suppose that  $\mathfrak{h} \in \mathcal{C}^1$  is a non-increasing function in the interval  $[-1, 0]$ . In particular, for  $s, \bar{s}$  as above we have  $\mathfrak{h}(\nu(s)) \leq \mathfrak{h}(\nu(\bar{s}))$ . Bearing these discussions in mind, the following inequality holds

$$- \frac{dz}{d\theta}(\bar{s}) = \frac{-4 \sin \theta(\bar{s}) \sqrt{1 + \tau^2 x(\bar{s})^2}}{8\mathfrak{h}(\nu(\bar{s})) - f(x(\bar{s})) \sin \theta(\bar{s})} < \frac{4 \sin \theta(s) \sqrt{1 + \tau^2 x(s)^2}}{8\mathfrak{h}(\nu(s)) - f(x(s)) \sin \theta(s)} = \frac{dz}{d\theta}(s), \quad (6.2)$$

and hence

$$z(s_0) - z(s_1) = - \int_{\pi}^{3\pi/2} \frac{dz}{d\theta} d\theta < \int_{\pi/2}^{\pi} \frac{dz}{d\theta} d\theta = z(s_0) - z(0);$$

i.e.  $z(s_1) > z(0)$  and no  $\mathfrak{h}$ -tori exist.

Note that the particular choice  $\mathfrak{h} = H_0 \in \mathbb{R}$  is compiled in this case, recovering the non-existence of rotational CMC tori in  $\mathbb{H}^2(\kappa) \times \mathbb{R}$ ,  $\text{Nil}_3$  and  $\widetilde{SL}_2(\mathbb{R})$ .

**6.2. Existence of rotational  $\mathfrak{h}$ -tori.** Finally, we exhibit the existence of rotational  $\mathfrak{h}$ -tori. The fact that  $\tau > 0$  has strong implications on the behavior of the angle function of a rotational  $\mathfrak{h}$ -surface. This, along with the arbitrariness of the prescribed function  $\mathfrak{h}$ , was the key that suggested us that the existence of rotational  $\mathfrak{h}$ -tori could be possible in these spaces.

Following the same notation as in Section 6.1, consider the compact piece of the  $\mathfrak{h}$ -nodoid generated by  $\alpha(s) = (x(s), 0, z(s))$  for  $s \in (0, s_1)$  and such that  $\theta(0) = \pi/2$ ,  $\theta(s_0) = \pi$  where  $x(s_0) := x_1$  and  $z'(s_0) = 0$ , and  $\theta(s_1) = 3\pi/2$ .

Again, since  $\theta'(s) > 0$  we express  $\nu(s)$ ,  $z(s)$  and  $x(s)$  as functions of the angle  $\theta$ . The motion of the orbits in the phase plane  $\Theta_{-1}$  implies that  $\nu(\theta)$  behaves as follows:  $\nu(\theta)$  is strictly decreasing for  $\theta \in (0, \pi/2)$ , and when reaches the value  $\theta = \pi$  it keeps decreasing until reaching a global minimum at some  $\hat{\theta} \in (\pi, 3\pi/2)$ . Then,  $\nu(\theta)$  is strictly increasing until reaching the value  $\theta = 3\pi/2$ , where it vanishes again.

Given  $\mathfrak{h} \in \mathcal{C}^1$ , we name  $I_1(\mathfrak{h}), I_2(\mathfrak{h})$  to the integrals of Equation (6.1) for the prescribed function  $\mathfrak{h}$ . Let  $H_0$  be a positive constant. Since Equation (6.2) holds for  $\mathfrak{h} = H_0$ , we conclude that  $I_2(H_0) > I_1(H_0)$ . Let us fix some  $\delta > 0$  small enough (we will determine later a bound for  $\delta$ ),  $x_1 > 0$  and define  $\nu_0 := -1/\sqrt{1 + \tau^2 x_1^2}$ . For each  $\lambda > H_0$ , consider the following function:

$$\mathfrak{h}_\lambda(y) = \begin{cases} H_0 & \text{if } y \in [-1, \nu_0 - \delta] \\ \lambda & \text{if } y \in [\nu_0, -\nu_0] \\ H_0 & \text{if } y \in [-\nu_0 + \delta, 1]. \end{cases}$$

If we prove that  $I_2(\mathfrak{h}_{\lambda_*}) < I_1(\mathfrak{h}_{\lambda_*})$  for some  $\lambda_* > H_0$ , by continuity we would have  $I_2(\mathfrak{h}_{\lambda_0}) = I_1(\mathfrak{h}_{\lambda_0})$  for some  $\lambda_0 \in (H_0, \lambda_*)$ , and hence we conclude the existence of an  $\mathfrak{h}_{\lambda_0}$ -torus. We prove this next.

We will denote with a sub-index  $(\cdot)_\lambda$  to the functions corresponding to the prescribed function  $\mathfrak{h}_\lambda$ , for each  $\lambda$ . Since  $\sin \theta > 0$  for  $\theta \in (\pi/2, \pi)$ ,  $x_\lambda(\theta) > x_0$ , and  $\mathfrak{h}_\lambda(\nu_\lambda(\theta)) = \lambda$ , the following holds

$$I_2(\mathfrak{h}_\lambda) = \int_{\pi/2}^{\pi} \frac{4 \sin \theta \sqrt{1 + \tau^2 x_\lambda^2}}{8\mathfrak{h}_\lambda(\nu_\lambda) - f(x_\lambda) \sin \theta} d\theta > \int_{\pi/2}^{\pi} \frac{4 \sin \theta \sqrt{1 + \tau^2 x_0^2}}{8\mathfrak{h}_\lambda(\nu_\lambda)} d\theta = \sqrt{1 + \tau^2 x_0^2} \int_{\pi/2}^{\pi} \frac{4 \sin \theta}{8\lambda} d\theta.$$

Hence,  $I_2(\mathfrak{h}_\lambda) \rightarrow 0$  as  $\lambda \rightarrow \infty$ .

On the other hand, let be  $\theta_1 < \theta_2 \in (\pi, 3\pi/2)$  such that  $\nu_{H_0}(\theta_i) = \nu_0 - \delta$ ; we choose  $\delta$  small enough so that the minimum of  $\nu_{H_0}$  is smaller than  $\nu_0 - \delta$ , hence  $\theta_i$  are well defined. So, we can split  $I_1(\mathfrak{h}_\lambda)$  as

$$- \int_{\pi}^{\theta_1} \frac{4 \sin \theta \sqrt{1 + \tau^2 x_\lambda^2}}{8\mathfrak{h}_\lambda(\nu_\lambda) - f(x_\lambda) \sin \theta} d\theta - \int_{\theta_1}^{\theta_2} \frac{4 \sin \theta \sqrt{1 + \tau^2 x_\lambda^2}}{8\mathfrak{h}_\lambda(\nu_\lambda) - f(x_\lambda) \sin \theta} d\theta - \int_{\theta_2}^{3\pi/2} \frac{4 \sin \theta \sqrt{1 + \tau^2 x_\lambda^2}}{8\mathfrak{h}_\lambda(\nu_\lambda) - f(x_\lambda) \sin \theta} d\theta.$$

Note that for  $\theta \in (\theta_1, \theta_2)$  in the second integral, the function  $\mathfrak{h}_\lambda(\nu_\lambda(\theta))$  is equal to  $H_0$ . In particular, all the geometric quantities appearing are the ones corresponding for the constant function  $H_0$ . Hence,

$$I_1(\mathfrak{h}_\lambda) > \int_{\theta_1}^{\theta_2} \frac{4 \sin \theta \sqrt{1 + \tau^2 x_\lambda^2}}{8\mathfrak{h}_\lambda(\nu_\lambda) - f(x_\lambda) \sin \theta} d\theta = \int_{\theta_1}^{\theta_2} \frac{4 \sin \theta \sqrt{1 + \tau^2 x_{H_0}^2}}{8H_0 - f(x_{H_0}) \sin \theta} d\theta = c_0 > 0,$$

where  $c_0$  is a positive constant that does not depend on  $\lambda$ .

Thus, for  $\lambda$  big enough we have  $I_1(\mathfrak{h}_\lambda) > I_2(\mathfrak{h}_\lambda)$ , hence there exists some  $\lambda_0 > H_0$  such that  $I_1(\mathfrak{h}_{\lambda_0}) = I_2(\mathfrak{h}_{\lambda_0})$ , i.e. there exist a rotational  $\mathfrak{h}_{\lambda_0}$ -torus.

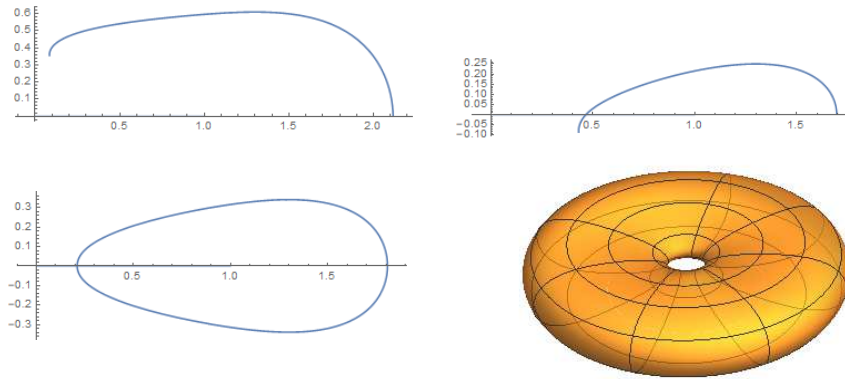


Figure 8: Top: the profile curves for different functions  $\mathfrak{h}_\lambda$ , for which  $I_1(\mathfrak{h}_\lambda) - I_2(\mathfrak{h}_\lambda)$  changes sign. Bottom: the profile curve and the rotational  $\mathfrak{h}$ -torus for a function  $\mathfrak{h}_{\lambda_0}$  such that  $I_1(\mathfrak{h}_{\lambda_0}) = I_2(\mathfrak{h}_{\lambda_0})$ . Here, the space is  $\text{Nil}_3$ .

## References

- [AbRo1] U. Abresch, H. Rosenberg, A Hopf differential for constant mean curvature surfaces in  $\mathbb{S}^2 \times \mathbb{R}$  and  $\mathbb{H}^2 \times \mathbb{R}$ , *Acta Math.* **193** (2004), 141–174.
- [AbRo2] U. Abresch, H. Rosenberg, Generalized Hopf differentials, *Mat. Contemp.* **28** (2005), 1–28.
- [Ale] A.D. Alexandrov, Uniqueness theorems for surfaces in the large, I, *Vestnik Leningrad Univ.* **11** (1956), 5–17. (English translation): Amer. Math. Soc. Transl. **21** (1962), 341–354.
- [Bue1] A. Bueno, The Björling problem for prescribed mean curvature surfaces in  $\mathbb{R}^3$ , *Ann. Glob. Ann. Geom.* **56** (2019), 87–96.
- [Bue2] A. Bueno, Half-space theorems for properly immersed surfaces in  $\mathbb{R}^3$  with prescribed mean curvature, *Ann. Mat. Pur. Appl.* **199** (2020), 425–444.

- [BuOr] A. Bueno, I. Ortiz, Invariant hypersurfaces with linear prescribed mean curvature, *J. Math. Anal. Appl.*, **487** (2020), DOI: <https://doi.org/10.1016/j.jmaa.2020.124033>.
- [BGM1] A. Bueno, J.A. Gálvez, P. Mira, Rotational hypersurfaces of prescribed mean curvature, *J. Differential Equations* **268** (2020), 2394–2413.
- [BGM2] A. Bueno, J.A. Gálvez, P. Mira, The global geometry of surfaces with prescribed mean curvature in  $\mathbb{R}^3$ , *Trans. Amer. Math. Soc.*, DOI: <https://doi.org/10.1090/tran/8041>.
- [Chr] E.B. Christoffel, Über die Bestimmung der Gestalt einer krummen Oberfläche durch lokale Messungen auf derselben, *J. Reine Angew. Math.* **64** (1865), 193–209.
- [Dan] B. Daniel, Isometric immersions into 3-dimensional homogeneous manifolds, *Comment. Math. Helv.* **82** (2007), 87–131.
- [DHM] B. Daniel, L. Hauswirth, P. Mira, Constant mean curvature surfaces in homogeneous manifolds, Korea Institute for Advanced Study, Seoul, Korea, 2009.
- [FeMi] I. Fernández, P. Mira, Constant mean curvature surfaces in 3-dimensional Thurston geometries. In *Proceedings of the International Congress of Mathematicians*, Volume II (Invited Conferences), pages 830–861. Hindustan Book Agency, New Delhi, 2010.
- [GaMi1] J.A. Gálvez, P. Mira, A Hopf theorem for non-constant mean curvature and a conjecture of A.D. Alexandrov, *Math. Ann.* **366** (2016), 909–928.
- [GaMi2] J.A. Gálvez, P. Mira, Uniqueness of immersed spheres in three-manifolds, *J. Differential Geometry*, to appear. [arXiv:1603.07153](https://arxiv.org/abs/1603.07153).
- [GaMi3] J.A. Gálvez, P. Mira, Rotational symmetry of Weingarten spheres in homogeneous three-manifolds, preprint, [arXiv:1807.09654](https://arxiv.org/abs/1807.09654).
- [Gor] C. Gorodski, Delaunay-type surfaces in the  $2 \times 2$  real unimodular group, *Annali di Matematica.* **180** (2001), 211–221.
- [GuGu] B. Guan, P. Guan, Convex hypersurfaces of prescribed curvatures, *Ann. Math.* **156** (2002), 655–673.
- [HsHs] W. T. Hsiang, W. Y. Hsiang, On the uniqueness of isoperimetric solutions and imbedded soap bubbles in non-compact symmetric spaces, *Invent. Math.* **85** (1989), 39–58.
- [LeRo] C. Leandro, H. Rosenberg. Removable singularities for sections of Riemannian submersions of prescribed mean curvature, *Bull. Sci. Math.* **133** (2009), 445–452.
- [LiMa] F. Martin, J. H. S. de Lira, Translating solitons in Riemannian products, *J. Differential Equations* **266** (2019), 7780–7812.
- [MePe] W.H. Meeks, J. Pérez, Constant mean curvature surfaces in metric Lie groups, in *Geometric Analysis*, **570**, pp. 25–110. Contemporary Mathematics, 2012.
- [Min] H. Minkowski, Volumen und Oberfläche, *Math. Ann.* **57** (1903), 447–495.

- 
- [PeRi] R. H. L. Pedrosa, M. Ritoré, Isoperimetric domains in the Riemannian product of a circle with a simply connected space form and applications to free boundary problems, *Indiana Univ. Math. J.* **48** (1999), 1357–1394.
- [Pip] G. Pipoli, Invariant translators of the Heisenberg group, preprint, [arXiv:1811.04619](https://arxiv.org/abs/1811.04619).
- [Pog] A.V. Pogorelov, Extension of a general uniqueness theorem of A.D. Aleksandrov to the case of nonanalytic surfaces (in Russian), *Doklady Akad. Nauk SSSR* **62** (1948), 297–299.
- [Tom] P. Tomter, Constant mean curvature surfaces in the Heisenberg group. *Proc. Sympos. Pure Math.* **54** (1993), 485–495.
- [Tor] F. Torralbo, Rotationally invariant constant mean curvature surfaces in homogeneous 3-manifolds. *Diff. Geo. Appl.* **28** (2010), 593–607.

The author was partially supported by MICINN-FEDER Grant No. MTM2016-80313-P and Junta de Andalucía Grant No. FQM325.